UNDERGRADUATE RESEARCH PROJECT

Prepared for: THE UNIVERSITY OF CAPE TOWN

Proper Orthogonal Decomposition - Based Material Parameter Identification

A Research Project in partial fulfilment of the requirements for a degree of
Bachelor of Science in Engineering
In the
Department of Civil Engineering

November 2015

Prepared by:
Simeon Solomons (SLMSIM002)

Supervisor:
Dr. Sebastian Skatulla

Plagiarism Declaration

I, Simeon Solomons, declare that this research project titled, ‘Proper Orthogonal Decomposition-Based Material Parameter Identification’ and the work presented in it are my own. I confirm that:

- I know that plagiarism is wrong. Plagiarism is to use another’s work and to pretend that it is one’s own.
- I have used the Harvard Convention for citation and referencing. Each significant contribution to and quotation in this report from the work or works of other people has been attributed and has been cited and referenced.
- This thesis is my own work.
- I have not allowed and will not allow anyone to copy my work with the intention of passing it as his or her own work.

Signature: _____

Date: _____

Abstract

With regard to efficiency in the design and manufacturing of structural elements it was found that understanding constitutive material laws is essential to civil engineers. When modelling engineering materials engineers face the task of making various assumptions including the choice of a material law applicable to their need. Furthermore, it should be noted that these assumptions affect the accuracy of constitutive material constants which not only influence the purpose for which said material could be used but in addition the economic value of the said material.

The use of Finite Element software could be employed and was found to be an important tool in reproducing environmentally accurate constitutive behaviour. This kind of software discretises a material specimen into finite elements in order to monitor different forms of constitutive behaviour. Moreover, the accuracy of this virtual environment is directly proportional to the amount of discretised elements a material is comprised of.

This research project aims to provide sufficient preliminary literature to cement the fact that computational methods should be used as reference in computing non-linear constitutive material parameters. This hypothesis is primarily based on the fact that numerous literature, which could be found in section 2, all come to the same conclusion. That is, as the complexity of a constitutive material law increases so does the time it takes to compute a solution from said law. This literature aims to identify methods that could be employed to minimize the simulation time of computing material constants from non-linear constitutive laws.

The distinctiveness of using the Proper Orthogonal Decomposition-based (POD) software ORION is that it reduces the complexity of a large dataset. It does so by using linear algebraic operations, namely Eigen vectors and their associated Eigenvalues, to project said dataset to a lower order solution space. In this lower order solution space ORION employs an interpolation technique in order to compute effective constitutive material constants. With regard to computational time, it should be noted that ORION could reduce simulation time greatly.

Furthermore, this work provides an outline of the hyperelastic and elastoplastic constitutive material laws and their respective constitutive models. The aforementioned material laws have been implemented within the framework of SESKA, Mesh free in-house software developed by Doctor Sebastian Skatulla, to analyse simple geometric layouts. Moreover, the author provides numerical examples in order to analyse these materials using in-house POD-based and SESKA software packages respectively.

Finally, this document provides the relevant preliminary conclusions with regard to the use of POD-based software and its effect on the simulation time of a non-linear constitutive material law. In contrast with coupling the Levenberg-Marquardt algorithm directly with the SESKA software package, the work in this research project is unique as it uses POD-based software as an intermediate software package in order to decrease computational simulation time.

Acknowledgements

Firstly, I would like to thank my Research Project supervisor, Dr. Sebastian Skatulla, for his emotional and mental support in the duration of this work. I would like to thank him for the provision of such an interesting topic. Furthermore, I would like to thank him for always setting aside time to explain numerous topics so that I could gain a better understanding of what was required. I could not have completed this research project without his guiding hand.

Secondly, I would like to express my gratitude to Ritesh Rama, a PhD candidate at the University of Cape Town. Ritesh compiled the in-house POD-based software ORION, without his expert input and knowledge of MATLAB I would not have been able to complete this research project. Additionally, I would like to salute him for running to and from computational mechanics lab and CERCAM labs, respectively, whenever I needed his assistance.

Thirdly, I would like to thank my colleagues, Mikael and Emmanuel, for providing an effective support structure for the duration of this Research Project.

My parents, for funding me throughout my university career. By providing an effective mental and emotional support structure, it was stressed that no matter how hard things got, I should never give up and keep moving forward. Furthermore, I would like to express many thanks to my sister Jesse-Mari, and my girlfriend Lisa for supporting me throughout my university career.

I would like to extend many thanks to Professor Robert Knutzen, for the provision of the basic knowledge on constitutive behaviour in the second year material science course (MEC2042F).

This Research Project has been supported by the Centre for High Performance Computing, Mowbray, without whom I would not have been able to complete my Research Project in the allocated time period.

Table of Contents

List of Figures

List of Equations

List of Tables

Glossary

CPU	Central Processing Unit
FEM	Finite Element Method
CEGM	Constitutive Equation Gap Method
RGM	Reciprocity Gap Model
EGM	Equilibrium Gap Method
VFM	Virtual Fields Method
POD	Proper Orthogonal Decomposition
PODI	Proper Orthogonal Decomposition with Interpolation
POM	Proper Orthogonal Modes
POV	Proper Orthogonal Values
MATLAB	Matrix Laboratory
GiD	Finite element software that could be used for pre-processing and post-processing of geometric models based in science and engineering
SESKA	Mesh free in-house software that could be used to analyse finite element models

1. Introduction

1.1 Background to this research project

For the purpose of this work, the researchable problem being investigated stems from the relationship between the choice of material law and its associated predicted structural behaviour. Material laws involve a range of constants that are used in the design and manufacture of numerous structures. These material constants do not necessarily apply to structural engineering only, but could also be applied to various fields of science and technology. An example of one such field is that of biomedical science, where the application of these constitutive material laws have been used to identify material parameters of the left ventricle of a human heart (Essack, 2014).

Constitutive laws can be broadly categorised into linear and non-linear laws, this research project, however, would focus on the latter in an effort to identify material parameters. The specific purpose of this research project is to provide and outline literature and numerical examples of materials exhibiting non-linear constitutive relations. Moreover, in concluding this research project the reader should have an understanding of how a MATLAB-based optimization algorithm could be coupled with in-house software to achieve the objective of material parameter optimization.

1.2 Justification of research project

To overcome the difficulty of approaching non-linear constitutive models analytically, one needs to think of applying an alternative approach to applying non-linear constitutive laws. The leading approach to applying analytical models, as described by Sanchez (2003), is that of computational programming that could be used to discretize structural elements into finite elements in order to accurately model the constitutive behaviour of said elements.

Moreover, for even the simplest structural element, analytically obtaining constitutive material constants from non-linear constitutive laws could be seen as being more complex and time consuming. The use of computational programmes to obtain constitutive material constants from non-linear constitutive laws could be seen as the way forward. From this standpoint, it could be seen that investigating how to use in-house software's such as SESKA and ORION to calibrate constitutive material laws would be important to model the behaviour of materials that exhibit non-linear constitutive behaviour.

Geometric modelling of structural elements will be done using finite element modelling software which would include simulating structural elements with user defined geometric layouts, support, loading conditions, and material parameters. Material parameter optimization will then be achieved by coupling in-house software ORION with a MATLAB-based Levenberg-Marquardt algorithm to further speed up computation time in obtaining constitutive material constants.

1.2.1 Problem Statement

Technology has advanced exponentially over the last 100 years and as a result of this, earth's populations, whether it be human or otherwise, need for more complex structures have become

more apparent to structural engineers. At present, structural elements are made up of a variety of materials such as metallic materials, polymeric materials, and composite materials. As the complexity of structural materials increase, as does the need to calibrate constitutive laws.

If a material exhibits linear constitutive behaviour, its constitutive material constants can be computed analytically without the need of high computing power. If, from the same experimental conditions, a different material exhibits non-linear behaviour, it would become more time consuming to compute constitutive material constants. From this standpoint, the need for calibrating non-linear constitutive parameters have become essential to model the mechanical behaviour of these structural materials. The specific problem to be studied involves the calibration of non-linear constitutive laws, which would be applied to specimens subject to simple tensile test procedure.

1.2.2 Determining material parameters

In the past, an inherent understanding of material parameters had been obtained by making various assumptions of real world engineering problems in order to simplify analysis of said problem. An example of an assumption used in engineering could be providing safety factors to ensure that Ultimate and Serviceability Limit State are satisfied, these factors are multiplied with applied loads to produce higher bending moments and shear forces which would in turn produce a slightly overdesigned structure.

Due to the increase in computing power, it has become apparent that analysing large scale engineering problems have become more frequent. For this, the use of Finite Element Modelling software such as SOFiSTiK, ABAQUS, GiD and many more could be used to mathematically model and solve real world engineering problems and systems in a virtual environment.

Along with the abovementioned software, Avril et al. (2008) emphasizes various methods that could be used to identify material parameters. For the purpose of this work, the updated method of inverse modelling was found to be an optimal method of obtaining non-linear constitutive material. This step-wise approach coupled with the comparison of experimental constitutive data and computer simulated constitutive data could be seen as being the preferred method, especially when it comes to complex problems.

Moreover, the updating method of inverse modelling should be coupled with the aforementioned optimization algorithm to obtain constitutive material constants. There are numerous algorithms that could be used with this approach but all come to the same conclusion; that being to locate the minimum, whether it be local or global, of real valued functions. Coleman, et al. (1999) discusses optimal ways to tackle the problem of nonlinearity would be to use a mathematical curve fitting method called the least squares method. This method could be used to determine an optimal solution by minimizing the sum of squares of a mathematical function (Coleman, et al. 1999).

Furthermore, once a simple structural element has been modelled while being subject to a user defined constitutive material law it could be further analysed using in-house software SESKA. Material parameters associated to user defined constitutive laws would then be defined in order to best fit experimental constitutive data. Previously in order to compute accurate constitutive material constants, SESKA would have been coupled with the MATLAB-based

Levenberg-Marquardt algorithm. A key drawback of the aforementioned method is that as the complexity of the constitutive law increases so does simulation time. For this, the in-house POD-based software ORION could be used as an intermediary programme to overcome the difficulties faced by coupling SESKA directly with a MATLAB-based Levenberg-Marquardt algorithm.

In order to use the in-house POD-based software ORION, SESKA needs to be used to populate a database results corresponding to varying material parameters, subsequently creating an envelope of simulated constitutive relations. This envelope of simulated data along with experimental constitutive data could then be used as input data for POD-based in-house software ORION for analysing purposes. Essentially, ORION then interpolates between different sets of result files to find the desired material constants that could be used in the design phase of structural elements.

1.3 Objectives of the Research Project

The objectives of this research project could broadly be categorized into two sections, primary objectives and secondary objectives. The primary objectives of this research project consist of familiarization with certain computer programmes and could be used in an attempt to achieve the ultimate goal of non-linear constitutive parameter optimization, these include:

- MATLAB, also known as Matrix Laboratory, is an interactive mathematical environment which would allow the user to analyse data, develop algorithms, and create models and applications (MathWorks Inc. 2015),
- GiD, this in-house software could be described as an interactive environment used to create finite element geometric models and produce input files for SESKA,
- SEKSA, which is a mesh free in-house software that could be used to analyse finite element models subject to varying constitutive material laws,
- ORION, this in-house software could be described as using reduced order methods to compute optimal material parameters.

In addition, secondary objectives of this research project consists of what is required to copiously investigate the POD-based material parameter optimization problem as set out as primary objectives. These include:

- Establishing a database of results associated to various constitutive material parameters, holding constant the constitutive law, geometric boundary conditions, and loading conditions
- Applying a material optimization methodology known as updating inverse modelling to a non-linear constitutive material law ,
- Using the MATLAB-based Levenberg-Marqaurdt optimization algorithm coupled with the in-house software ORION to provide optimal constitutive material parameters.

1.4 Scope of investigation

This research project aims to provide an investigation into the calibration on non-linear constitutive material laws and the importance thereof in the context of Civil Engineering. With this intention, understanding the influence of constitutive laws and their associated influence on material choice is of great importance when designing and maintaining structural developments.

In order to compute the aforementioned material constants, simple geometric models of material specimens subject to a uniaxial tensile load will be created and analysed. This research project aims to study the effects of how an increase in the complexity of constitutive laws would not affect the simulation time of producing common constitutive constants such as; Young's Modulus, Poisson's Ratio, shear modulus and yield stress when coupling in-house POD-based software with a MATLAB-based Levenberg-Marquardt algorithm.

1.5 Layout of this document

This research project will outline the requirements needed for an investigation into the use of two material laws that could be implemented to model, analyse, and compute non-linear constitutive material parameters. This section will outline the layout of this literature review with regard to what will be addressed in each chapter.

In section 1, this research project provides an introduction to *Proper Orthogonal Decomposition-based Material Parameter Optimization* and provides the reader with the relevant background to how this topic will be incorporated to investigate the workings of non-linear constitutive material laws and their associated parameters.

In section 2, this document contains a literature review of available peer reviewed articles, journals, and books relevant to this research project. It includes a literature review of defining various constitutive material laws and how non-linear constitutive material laws could be implemented in the ultimate objective of *Proper Orthogonal Decomposition-based Material Parameter Optimization.* Furthermore, in this literature review it was found that simple uniaxial tensile tests on vulcanised rubber would produce homogenous non-linear stress-strain relations. This discovery proved to be useful as it was used to familiarize oneself with computer programs mentioned in section 1.3. Once the primary objectives was complete, a study into the elastoplastic behaviour of a ductile metal subject to uniaxial tensile loading could be done.

In section 3, this document outlines the computational mechanics theory relevant to the work being studied. Furthermore, this section outlines how important continuum mechanics is in the context of engineering works and the balance laws of said topic which are important to this work. Finally, this section concludes by providing the reader with definitions of the appropriate equations which could be used to construct general constitutive material models.

In section 4, this document provides a detailed description of material laws applicable to this research project. This section includes defining and comparing various hyperelastic constitutive material laws which would give the reader a better understanding of how the author came to the conclusion of using the neo-Hookean hyperelastic material law for analysing vulcanized rubber. Moreover, this section would provide the reader with an improved understanding of two significant yield criterions used to model the elastoplastic behaviour of ductile metals subject to uniaxial tensile loading.

In section 5, this document provides numerical examples of simple geometric layouts. This includes a comparison between experimental and simulated constitutive data to obtain the ultimate goal of material parameter optimization. Subsequently, this section concludes by providing optimal material constants that could be used for modelling the mechanical behaviour of a rubber-like and titanium specimen, respectively, under simple tensile loading.

Finally, section 6 provides relevant conclusions the author has come to in the duration of this research project. Furthermore, this section will provide an outline into the efficiency of using Proper Orthogonal Decomposition-based Material Parameter Optimization to obtain non-linear constitutive material constants.

2. Literature review

2.1 Constitutive Laws

2.1.1 Introduction

Common to all mechanical analysis of engineering materials and their associated behaviour in structural components, is the need for constitutive models that link the states of stress and strain (Runesson, 2006). From this standpoint, it could be seen that constitutive equations form a vital part in the design phase of a structural engineering project. Maintaining a similar geometric layout, support, and loading conditions it could be seen that these laws and their associated equations could provide a method of computing optimal constitutive material parameters.

In recent times, numerous engineering materials have been used for the design and manufacture of structural elements. By logic and reasonable knowledge of engineering concepts, it would imply that different materials, such as concrete and metals, would make use of different constitutive laws. William (2002) states that this is primarily due to the fact that engineering materials would exhibit different stress-strain relationships, even though said materials were to have a similar geometric layout, loading and support conditions. This finding is associated to a difference in the microstructure of an element, which could be seen in Figure 2-1, and would cement the fact of a difference in material behaviour in response to similar loading conditions.

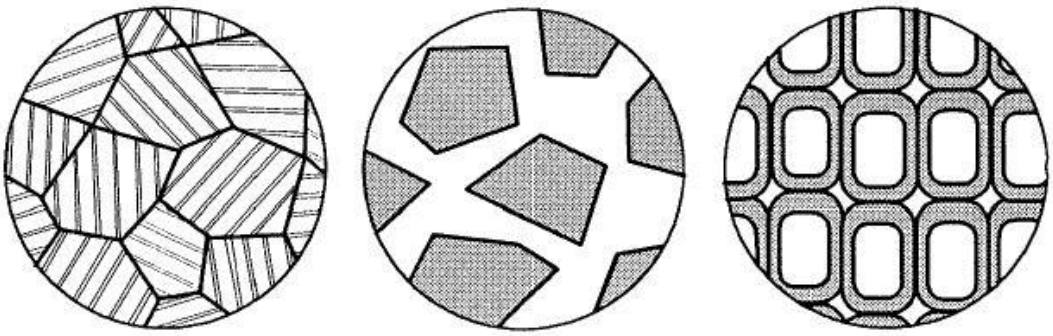

a) b) c)

Figure 2-1: Typical microstructure of (a) wood, (b) Concrete, and (c) Wood (Runesson, 2006)

William (2002) further states that despite this discovery, one could still apply the same basic principles and concepts in establishing constitutive relations. From this, it would imply that the only difference comes from implementing these constitutive laws. Using ductile metal as an example, a linear constitutive law could be used to model and obtain material parameters for said material in the region where it exhibits elastic behaviour or the use of a non-linear constitutive law to model and obtain material parameters in the region where the material exhibits plastic behaviour.

2.1.2 Methods of applying Constitutive Laws

The difference in material behaviour does not only stem from the differences in the

microstructure of the material in question, it generally stems from the intended use for said material. Figure 2-2 displays the different scales that could be applied to different constitutive models, where the structural mechanics and macro mechanics level apply to civil engineering problems and laboratory experimental results, respectively.

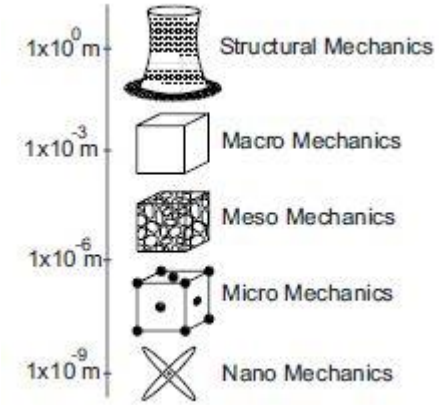

Figure 2-2: Scales of material mechanics (William, 2002)

Furthermore, there are numerous methods of applying constitutive laws, all of which have one strategic advantage. As outlined by Runesson (2006), these laws follow the same basic principles while the conceptual approaches could be divided into three broad categories:

- Fundamental approach: this method requires that the user has an intrinsic understanding the behaviour of a structural element with regard to deformation and failure characteristics. The primary characteristic of this approach is that it focuses more on micromechanical behaviour to establish constitutive relations.
- Phenomenological approach: this approach concentrates more on the macroscopic level and is carried out by comparing user defined experimental results with computer simulated results.
- Statistical approach: these methods are not normally used for predicting material behaviour, this is due to the fact that it could only be used as response functions for specific loading and environmental conditions. In the context of science and technology, and even more specific in engineering, we're more focused on studying a general problem instead of a specific problem.

2.1.3 Constitutive Laws in the Context of this Research Project

In accordance with the objectives set out in section 1.3, it could be seen that this work would make use of the phenomenological approach to apply material optimization methodology known as inverse modelling. This approach involves minimizing an objective function made up of the difference between the user defined experimental results and computer simulated results. These results could be observable material constants such as elasticity, stress, strain, temperature and so on (William, 2002).

In this work, it was found that subjecting a polymeric material, such as rubber, to a uniaxial tensile load would produce a homogenous stress-strain relationship which could be used as an initial comparison to obtain optimal material parameters. Once material constants of rubber

subject to a uniaxial tensile load has been computed with confidence, a possible material that exhibits a more complex constitutive relationship could be analysed.

For this, the use of a titanium specimen subject to similar experimental conditions to that of rubber could be analysed. The lone difference between these materials is the constitutive material law being implemented. The former material's constitutive model will be centred on creating a constitutive model using the neo-Hookean law of hyperelasticity while the latter material would make use of von Mises yield criterion, respectively, to obtain optimal material parameters.

2.2 Constitutive relations of materials being investigated

2.2.1 Elastoplastic materials

As mentioned in section 2.1, the need for constitutive models that link stress and strain are of chief importance when it comes to analysing engineering materials. Stress-strain diagrams come in a variety of shapes and forms, this stems from a diversity of interlinking variables such as how the material is manufactured, the rate of loading, the time period of testing and so on (Hibbeler, 2008). This section will include definitions of stress and strain, a brief description of a conventional stress-strain diagram and how these diagrams will relate to the calibration of non-linear constitutive material laws.

Introduced in the second year civil engineering undergraduate course called Material Science (MEC2042F), stress and strain are material parameters that could be obtained experimentally in a controlled environment, using stress and strain gauges respectively. Analytically, engineering stress is generally defined as the force per cross-sectional area and could be defined as:

$$\sigma = \frac{P}{A_0} \qquad \text{Equation 2-1}$$

Where σ denotes the stress tensor, P is the applied load, and A_0 is the specimen's original cross-sectional area. From Equation 2-1, one could deduce that stress is directly proportional to the applied load and indirectly proportional to its cross sectional area. Consequently, as the original cross sectional area of a material specimen remains constant while the applied load to said specimen changes, the stress tensor obtained from this calculation will change by the same percentage.

By the same manner, engineering strain could generally be defined as the ratio between the changes in a material specimen's length to the length of the original material specimen and could be expressed as:

$$\epsilon = \frac{\delta}{L_0} \qquad \text{Equation 2-2}$$

Where ϵ represents the strain constant, δ represents the change in a specimens' length due to applied loads, and L_0 represents the specimens' original length. As with stress, the relationship between strain and its parameters are such that it is directly proportional to the change in the tested specimens' length and indirectly proportional to the tested materials' original length. To

better interpret the relationship between stress and strain Figure 2-3 displays a conventional and true stress-strain diagram for a ductile engineering material, namely titanium, subject to a uniaxial tensile load.

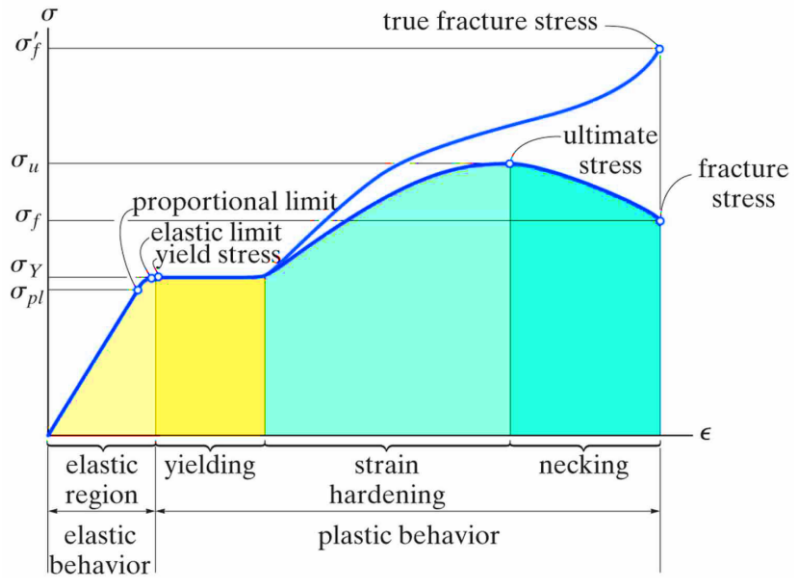

Figure 2-3 : Conventional and true stress-strain diagram for a ductile metal (Hibbeler, 2008)

Referring to Figure 2-3, the elastic region is where a load could be applied to a specimen and once said load is removed, the material will return to its original geometry. In the elastic region the ratio of stress to strain is linear and could be termed Young's modulus of elasticity. This linear relationship was discovered by Robert Hook in 1676 and further modified by Thomas Young in 1807, after which the ratio was so named (Hibbeler, 2008). Young's modulus of elasticity could generally be expressed as:

$$E = \frac{\sigma}{\epsilon} \qquad \text{Equation 2-3}$$

Once a material goes beyond its elastic limit it starts exhibiting plastic behaviour which, in the context of this research, could be described as non-linear constitutive behaviour. In this region the material starts to permanently deform without any increase in applied loads. Once the material has yielded it undergoes strain hardening, which means that the material could be subject to higher applied loads that it originally experienced in the elastic region. Figure 2-3 shows that strain hardening would only last up until a certain point, namely the ultimate stress, after which the material would start to fail in its ultimate objective of resisting an applied load.

One of the secondary objectives mentioned in Section 1.3 states that this research project aims to use inverse modelling to calibrate non-linear constitutive laws and obtain material constants from these laws. To thoroughly investigate non-linear behaviour of the structural material in question, one has to look at the stress-strain response of said material when subjected to a particular load. Structural loads could be arbitrarily placed to investigate different stress-strain responses but, in the context of this research and in order to obtain a simplified desired output, loads should either act axially to create tension. As the stress-strain behaviour has been discussed in this section, the following section will briefly investigate stress-strain responses of polymeric material specimens, which inherently exhibit nonlinear constitutive behaviour when

subject to uniaxial tensile loads.

2.2.2 Hyperelastic Materials

As discussed in section 2.1.3, a rubber-like material subject to uniaxial tensile loads has been chosen as an initial material to calibrate simulated constitutive parameters to experimental results as rubber materials exhibit highly non-linear constitutive behaviour (Guo & Sluys, 2008). Microscopically, rubbers are made up of many identical chemical units that are joined together to make up giant molecules (Material science module 5, 2012). Rubbery materials fall under the classification of polymeric materials which could broadly be classified into three categories namely; thermoplastics, thermosets, and elastomers. The only difference between these categories stems from the structure, properties, and use of such materials.

Figure 2-4 shows the microscopic behaviour of a typical rubbery polymeric material when subjected to uniaxial tensile loads, where part a) represents the material in its natural state while part b) represents the material under the applied loading.

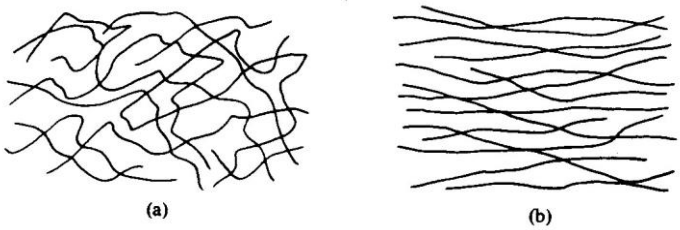

Figure 2-4 : Microscopic behaviour of rubbery polymeric materials subject to tensile loads (Department of Chemistry and Biochemistry, University of Colorado Boulder, 2015)

Although rubbery materials exhibit linear behaviour on a microscopic level, Hui et al. (2010) states that when a load is applied to a rubbery polymeric test specimen its macroscopic stress-strain diagram looks like the one found in Figure 2-5.

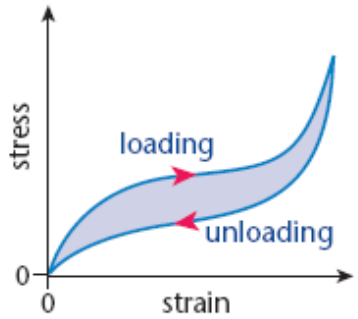

Figure 2-5: Macroscopic stress-strain diagram of loading and unloading a natural rubber specimen (World, 2015)

Along with Hui et al. (2010), Taber (2004) and Bigoni (2012) came to the same conclusion with regard to hyperelastic materials. A hyperelastic material is a material for which the constitutive relationship of stress and strain could be derived from a strain-energy density function. Numerous material laws that could be applied to obtain constitutive material parameters from hyperelastic materials are outlined in Bigoni (2012) namely; the Kirchhoff-Saint Venant, neo-Hookean, Mooney-Rivlin, Arruda-Boyce, and Gei-Bigoni-Guicciardi material model (also referred to as

GBG approach).

As described by Bigoni (2012), the Kirchhoff-Saint Venant and neo-Hookean material models could be seen as the simplest constitutive equations to analyse and could be used to model materials from their unloaded state until they reach their rupture point. Furthermore, it should be noted that the GBG approach could only be used for quasi-brittle materials such as concrete and soil, thus it will not be investigated as it falls outside the scope of this research project.

From this standpoint, the author selects the Kirchhoff-Saint Venant approach to modelling and analysing the constitutive response of rubber subject to uniaxial tensile loading. Numerical simulations of rubbery materials using this hyperelastic material law will be investigated as a precursor to the more complex constitutive behaviour of an elastoplastic material. It should be noted that the latter material would be subject to similar loading and boundary conditions as the former material. Moreover, the chosen elastoplastic material would only be calibrated up until its ultimate tensile strength, since the framework of SESKA's does not implement the behaviour of such materials at rupture.

2.3 Inverse Modelling

2.3.1 Introduction

Constitutive parameter identification could often be referred to as an inverse problem, this iterative technique takes into account deformation, support, and geometric boundary conditions of the experimental set up (Avril et al, 2008). Material laws are the most important factor in modelling the mechanical behaviour of monolithic, as well as composite structures. According to Hibbeler (2008) these material laws involve a range of material constants such as Young's Modulus and Poisson's ratio, which describes the stress-strain ratio otherwise known as elasticity and the ratio of a change in length between lateral and longitudinal length when a material is being stretched respectively.

The subsequent sections would provide a summary of how inverse modelling will be used to calibrate non-linear constitutive material laws. On the subject of inverse modelling, it is important to note that this technique could broadly be split into two distinct methods; updating methods and non-methods of inverse modelling.

2.3.2 Methods of Inverse Modelling

Updating methods of inverse modelling involve using an initial assumption of constitutive parameters and focus on numerically computing displacement, deformation, and stress fields at the area of interest (i.e. at some point of a structural element, such as a beam). For this method of inverse modelling, full-field measurements are useful but not required which is advantageous to the user (Avril et al, 2008).

The primary task of an updating method of inverse modelling is to minimize an objective cost function, a description of which could be found in Section 2.3.3. With regard to non-linear constitutive material laws, cost functions could be better explained as the quadratic deviation between defined experimental results and computer simulated results (Essack, 2014). To achieve minimization of this cost function and obtain the desired material parameters, an optimization

algorithm needs to be established and integrated into this method of inverse modelling. Moreover, figure 2-6 shows a schematic of the updating method of inverse modelling adapted in this work. One major disadvantage is that updating methods of inverse modelling are CPU intensive, thus stating that an average desktop computer would be inadequate to compute the desired material parameters thus making the need for modified CPU devices apparent. Such CPU devices will be provided by Dr. Skatulla for the duration of this research project.

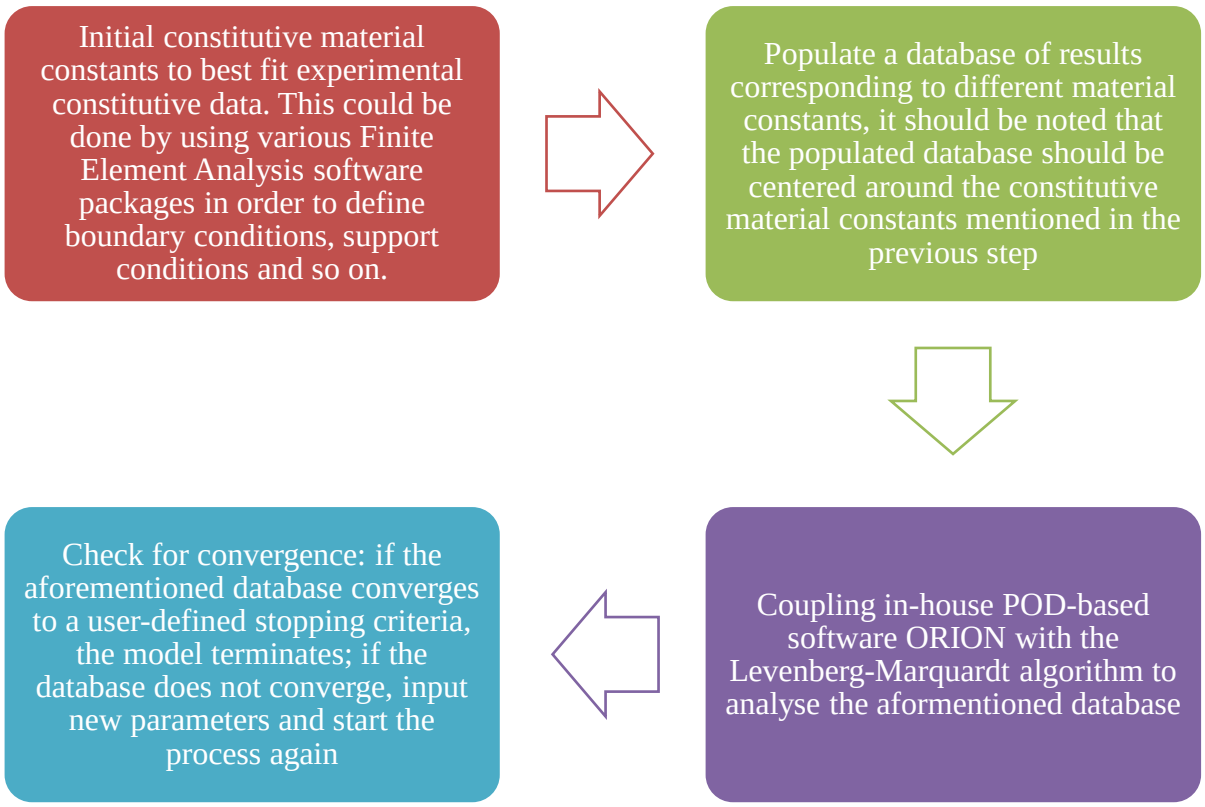

Figure 2-6: Schematic of the updating method of inverse modelling with regard to this work

Furthermore, there are numerous numerical methods that use the updating method of inverse modelling. These numerical methods, as outlined Avril et al. (2008), make use of different approaches to obtain their ultimate goal of optimizing an objective cost function and could be summarized as follows:

- Finite Element Method (FEM): this form of numerical simulation involves the coupled use of the Finite element software package to discretise a structural specimen into finite elements and provide the best possible comparison between defined experimental results and computer simulation results.
- Constitutive Equation Gap Method (CEGM): this method works in conjunction with Finite Element Methods, thus it is not a stand-alone method. It serves as a means of creating more accurate Finite Element Models by smoothing meshes to minimize the constitutive gap between defined experimental results and computer simulation results

and would provide more accurate material parameters.

- Reciprocity Gap Model (RGM): the outstanding attribute of this method, which could also be seen as its primary drawback, is that full-field measurements are needed to compute the desired material parameters and hence for the purpose of this work this method will be ignored.

In contrast to updating methods of inverse modelling, non-updating methods assume that constitutive parameters of the investigating problem instead of striving towards them. This could be achieved by means of evaluating computer simulated results with experimental results, note the omission of the term "user defined", where the latter depends on the assumed constitutive parameters while the former does not. From this statement, it could be seen that this method requires the use of a priori knowledge which would effectively limit the use of this method to technically inclined users for achieving optimal results.

The primary advantage of this method is that it is less CPU intensive than that of updating methods of inverse modelling, since non-updating methods make use of full-field data and equilibrium equations to provide a more accurate solution to the problem being investigated. A Finite Element approach, along with two more approaches, could be used in the numerical simulation of non-updating method of inverse modelling. These non-updating methods were outlined in Avril et al. (2008) and could be summarized as follows:

- Equilibrium Gap Method (EGM): this method is based on the discretization of equilibrium equations, it does this to achieve a similar result to that of CEGM, to minimize the equilibrium gap between simulated results and experimental results of a diverse set of fields(i.e. stress, strain, and so on)
- Virtual Fields Method (VFM): this is one of the more common methods of obtaining displacements and deformation. An advantage of this method is that it could be done analytically by means of standard polynomial functions. The ultimate drawback is that it requires full-field measurement data.

Consequently, since simulated constitutive data would be compared to experimental constitutive data using finite element software, the updating method of inverse modelling would be the optimal method of inverse modelling. According to Avril et al. (2008), most finite element software packages are coupled with the principle of virtual work which will be further detailed in section 3. The primary advantage of this is that these software packages could easily be used to analyse linear and non-linear constitutive relations.

2.3.3 Objective Cost function

In section 2.3.2, the updating method of inverse modelling had been identified as an optimal method of obtaining constitutive parameters from non-linear constitutive relations. During the course of preparing this literature review, it was found that minimizing an objective cost function was emphasized to be at the crux of these updating methods. This section will discuss two broad categories of objective cost functions namely, single objective cost functions and multiple (or multi-) objective cost functions.

As the terms single and multiple suggest, a single objective functions ultimate goal is to find an optimal solution between the minimum and maximum value of a single function. In contrast, a multi-objective function serves to find an optimal solution by identifying, grouping,

and comparing many single objective functions (Savic, 2002).

Although applying single objective cost functions would seem more advantageous as it could form the framework of a multi-objective framework, the foremost drawback of applying a single objective cost function as described by Savic (2002) is that it does not provide a set of alternate solutions that trade different objectives against one another. In contrast, multi-objective cost functions provide a more accurate solution by providing a range of alternatives that delivers a trade-off between different objectives.

As with single objective cost functions, multi-objective cost functions have a chief drawback which stems from a problem where the single objectives that make up a multi-objective framework could conflict with one another, this phenomenon is called the Pareto optimality (Lin & Zhang, 2008). Conflicts usually arise due to the fact that certain objectives cannot minimize and maximize at the same time, this is illustrated in Figure 2-7 which shows a typical bi-objective cost function.

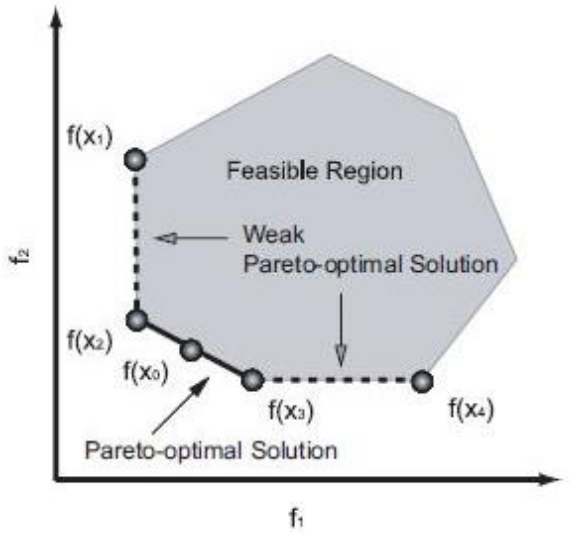

Figure 2-7: Geometric illustration of the Pareto Optimality (Savic, 2002)

From Figure 2-7 it could be seen that the dotted lines from $f(x_1)$ to $f(x_2)$ and $f(x_3)$ to $f(x_4)$ show minimum values of the functions f_1 and f_2 respectively. To obtain an accurate solution an average between these values needs to be established to obtain an optimal solution for both objectives. Hence, a set of Pareto-optimal solutions can be seen by means of the solid line running from $f(x_2)$ to $f(x_3)$. In the context of this research the concept of Pareto Optimality cannot be used since it presents an infinite number of solutions instead of a unique solution, of which the latter is needed to obtain desired material parameters.

A common approach to overcome this anomaly would be to simply introduce a weighted sum approach. This approach combines the objective vectors that make up a multi-objective cost function by multiplying each vector with an appropriate scalar with the aim of minimizing the overall multi-objective cost function and hence obtain optimal material parameters (Coleman, et al, 1999). As with all weighting methods the primary drawback of using this method is that using different scalars would produce different solutions. To overcome this disadvantage, Gennert &

Yuille (1998) explains how to find optimal weights by using the min-max principle which would be more beneficial for non-linear constraint methods. Another key disadvantage of the weighted method doesn't concern the method itself, rather it concerns the shape of the region wherein the solution lies. Since the weighted method operates by moving a weighted multi-objective function to a point where it touches a convex feasible region A, which could be seen in Figure 2-8.

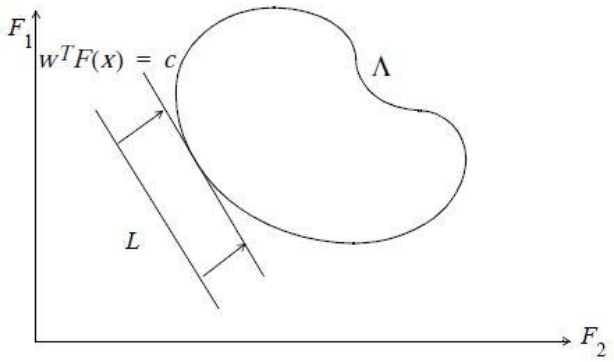

Figure 2-8: Geometric Interpretation of the Weighted Sum Method (Coleman, et al. 1999)

If said solution space has a subspace(s) that are not convex, another method needs to be introduced to overcome this variance. For this, a method called the $\in$-Constraint method could be introduced which would overcome the non-convexity problem that the weighted method could be subject to (Coleman, et al. 1999)

Coleman et al. (1999) discusses how the $\in$-Constraint method obtains solutions from a solution space that has non-convex subspaces and could be geometrically summarized in Figure 2-9.

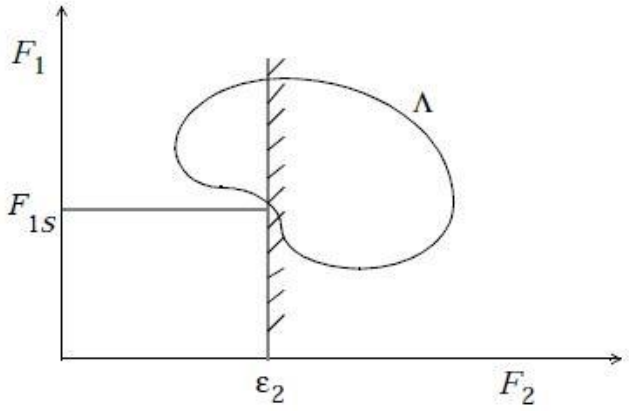

Figure 2-9: Geometric interpretation of the $\in$ - Constraint Method (Coleman, et al. 1999)

From Figure 2-9 it could be seen that one function, let's call this the primary function, needs to be minimized while subjecting all the other functions that make up the multi-objective cost function to an inequality for a known constraint, $\in$. Furthermore, to obtain an optimal value of $\in$, knowledge on the branch of statistics known as decision theory needs to be attained which falls outside the scope of this research project (Essack, 2014). Consequently, the preferred

method of obtaining the solution to a multi-objective cost function in the context of this research would be the weighted sum method.

2.3.4 Material Parameter Identification

As mentioned in section 2.3.3, the root of updating inverse techniques is minimization of a cost objective function. To achieve this, an optimization algorithm needs to be established. Throughout the course of the research done for this literature review, many such algorithms were found and could broadly be categorized into two distinct sections, namely: Gradient based algorithms and Non-gradient based algorithms. (Coleman, et al. 1999)

The chief difference between these methods are their respective rate of convergence from initial values to desired values. Coleman, et al. (1999) states that gradient-based algorithms such as the Gradient algorithm, Gauss-Newton algorithm, and the Levenberg-Marquardt algorithm are characterized with having faster convergence towards obtaining a desired set of parameters. It should be noted that with Levenberg-Marquardt algorithm is a combination of the Gradient algorithm and the Gauss-Newton algorithm (Lourakis, 2005). These algorithms however, are not without their drawbacks, gradient based algorithms strongly depend on set of initial parameters and could easily fall into local minimums when dealing with multi-objective cost functions.

By way of contrast, non-gradient based algorithms such as particle swarm algorithms and genetic search algorithms are characterized by having slower convergence properties to a desired parameter set. Non-gradient based algorithms to not inherently depend on an initial parameter set, rather they depend on the existence of said initial set of parameters (Eberhart & Kennedy, 1995). As Eberhart & Kennedy (1995) explains, Non-gradient algorithms are less CPU intensive and extremely simple to implement but they do have a chief drawback in that they are not as focussed on non-linear least squares curve fitting which contrasts Gradient-based algorithms.

Furthermore, it was found that the Levenberg-Marquardt algorithm was best suited to minimize the chosen method of using multi-objective cost function. This least squares method could be used for calibrating linear and non-linear constitutive laws, of which it is best suited for the latter (Coleman, et al. 1999). This algorithm operates by using an iterative technique called the search direction technique to obtain a solution of a set of linear equations. The distance from an initial parameter set and the desired parameter set determines the behaviour of this algorithm. When the initial parameter set is not in the vicinity of a feasible solution space the algorithm behaves like the gradient method, and when the initial parameter set is in the vicinity of a feasible solution space it behaves like the Gauss-Newton algorithm. Moreover, the Levenberg-Marquardt algorithm could be categorized into two broad categories namely, the constrained method and the projected method.

According to Kanzow & Petra (2005), the methods have the same convergence properties with the only difference being how they arrive at the desired set of material parameters. The constrained method solves strictly convex minimization sub problems, thus making it more CPU intensive to compute. While the projected method linearizes an initial set of parameters by projecting them onto a feasible solution space, making it easier and faster to compute the desired set of parameters. Consequently, the projected version of the Levenberg-Marquardt algorithm has been selected as the optimization algorithm to minimize the multi-objective cost function as set out in Section 2.3.2 and will be further detailed in the research project.

2.4 Reduced Order Methods

2.4.1 Introduction

The use of POD-based software stems from the fact that, the simulation time of the iterative techniques proposed in the abovementioned sections tend to increase as the complexity of a constitutive law increases. To overcome this hindrance, a MATLAB-based Levenberg-Marquardt algorithm will be coupled with in-house POD-based software ORION. The subsequent sections will briefly describe what POD is and how a similar version of this method will be used to decrease simulation time. It should be noted that the methods proposed in this section were adopted form Rama & Skatulla (n.d.), Lin & Zhang, 2008, and Ly & Tran (2001) and was not developed by the author.

2.4.2 Proper Orthogonal Decomposition

POD is a reduced order method which, as the name suggests, reduces the complexity of large data set. It does so by projecting said data onto a subspace made by proper orthogonal modes, which could be mathematically interpreted as eigenvectors. Furthermore, the values corresponding to these modes indicate the level of importance of each proper orthogonal mode (Lin & Zhang, 2008). With regard to increasing the accuracy of the POD method, the choice of proper orthogonal modes are important. For this, Kerchen et al. (2005) proposes the use of proper orthogonal values, which could mathematically interpreted as eigenvalues such that each proper orthogonal mode corresponds to a particular proper orthogonal value.

POD provides an efficient way of capturing the dominant components of a large data set, by means of reducing said data field to a finite number of Eigen functions (Lin & Zhang, 2008). This method, however, is not without its drawbacks. According to Ly & Tran (2001) the POD method assumes that any problem could correspond to a mathematical model however, in the field of structural engineering certain data fields may not be well-defined and it would be too complicated to obtain optimal solutions from a generated data set. Consequently, for the purpose of this research project it was found that a variation of POD known as PODI could be employed to overcome this assumption entirely.

An important prelude to the mathematical derivation of the POD method is that of establishing a data matrix U, which is comprised of a set of displacement fields and could be expressed as

$$\boldsymbol{U} = \{\boldsymbol{u}^1, \boldsymbol{u}^2, \ldots\ldots, \boldsymbol{u}^n\} \qquad \text{Equation 2-4}$$

Where the superscript of $\boldsymbol{u}$ denotes the number of discrete time steps. It should be noted that the number of time steps n << m, where m refers to the number of displacement degrees of freedom. Moreover, the individual displacement vectors could be expressed as

$$\boldsymbol{u}^i = \sum_{j=1}^{n} \alpha_j^i \boldsymbol{\psi}_j \qquad \text{Equation 2-5}$$

Where ψ denotes a set of basis vectors and α are coefficients. Moreover, *i* denotes the number of time steps and *j* refers to the number of basis vectors. Consequently, using the Karhunen-Lo`eve decomposition method to maximise the projection of $\boldsymbol{u}$ onto solution space $\boldsymbol{\phi}$, an orthogonal constraint needs to be established such that $\|\boldsymbol{\psi}\|^2 = 1$:

$$max_{\psi} = \langle |\boldsymbol{U}, \boldsymbol{\psi}|^2 \rangle \qquad \text{Equation 2-6}$$

Using the Lagrange multiplier method the following Eigen value expression could be obtained

$$(\boldsymbol{R}, \boldsymbol{\psi}) = \boldsymbol{\lambda\psi} \qquad \text{Equation 2-7}$$

With $\boldsymbol{R} = \frac{1}{n}\boldsymbol{U}\boldsymbol{U}^T$producing a positive semi-definite symmetric matrix. While $\boldsymbol{\lambda}$ and $\boldsymbol{\psi}$ would refer to Eigen values and Eigen vectors respectively. Consequently, if the data matrix **U** is very large the resulting matrix **R** could also be seen as being very large which would increase computation work to find solutions for $\boldsymbol{\lambda}$ and $\boldsymbol{\psi}$**.** For the sake of overcoming this problem, the snapshot method proposed by Sirovich (1987) is commonly used. Consequently, decrease the size of the aforementioned matrix, equation 2-7 could be modified to the form of

$$(\boldsymbol{C}, \boldsymbol{\xi}) = \boldsymbol{\lambda\xi} \qquad \text{Equation 2-8}$$

With a new positive semi-definite symmetric matrix $\boldsymbol{C} = \frac{1}{n}\boldsymbol{U}^T\boldsymbol{U}$ which would be defined in terms of Eigen values. It should be noted, however, that the associated Eigen vectors are not proper orthogonal modes. In order to circumvent this problem, Li et al. (2011) proposes the following equation

$$\boldsymbol{\psi^i} = \frac{\mathbf{1}}{\sqrt{\mathrm{n}\boldsymbol{\lambda}_i}}\boldsymbol{U\xi^i} \qquad \text{Equation 2-9}$$

Furthermore, to preserve the energy of the dataset ***U*** when it is being reduced from a higher order solution space to a lower order solution space, Falkiewicz & Cesnik (2011) proposes the following expression

$$\varepsilon_{rel} = \frac{\sum_{g=1}^{n-r}\lambda_f}{\sum_{g=1}^{n}\lambda_f} \times 100 \qquad \text{Equation 2-10}$$

Where r is the number of proper orthogonal modes conserved and r < n. Finally, Lin & Zhang (2008) suggests that in order to conserve the greatest amount of energy the proper orthogonal modes associated to the highest proper orthogonal values should be selected to obtain optimal solutions.

2.4.3 Proper Orthogonal Decomposition with Interpolation

For the purpose of this work, the use of POD based in-house software ORION would be used to overcome extended simulation time associated with the repetitive equation assembly used to compute constitutive material constants. The basis of the POD method is that it compresses a series of data sets such that the new solution space is much smaller than the original solution space. It should be noted that the methods proposed in this section was adopted form Ly & Tran (2001) and Lin & Zhang (2008), and was not developed by the author.

The basis of the PODI method employed by in-house software ORION is that it compresses a series of data sets for interpolation (Lin & Zhang, 2008). This data matrix $\boldsymbol{U}$ would be comprised of varying results corresponding to different material parameters. This in-house software then employs an interpolation technique called the Moving Least Squares (MLS) method in order to find optimal material parameters.

According to Rama & Skatulla (n.d.), the mathematical derivation of the PODI method starts with an expansion of the matrix described in equation 2-4, and could be expressed as

$$\begin{bmatrix} u_1^1 & \cdots & u_1^n \\ \vdots & \ddots & \vdots \\ u_m^1 & \cdots & u_m^n \end{bmatrix} \approx \begin{bmatrix} \phi_1^1 & \cdots & \phi_1^n \\ \vdots & \ddots & \vdots \\ \phi_m^1 & \cdots & \phi_m^n \end{bmatrix} \begin{bmatrix} \alpha_1^1 & \cdots & \alpha_1^n \\ \vdots & \ddots & \vdots \\ \alpha_m^1 & \cdots & \alpha_m^n \end{bmatrix} \qquad \text{Equation 2-11}$$

Considering an arbitrary displacement vector $\boldsymbol{k}$ (where k < n), basic linear algebra techniques could be employed to describe this displacement vector as

$$\begin{bmatrix} u_1^k \\ u_2^k \\ \vdots \\ u_{m-1}^k \\ u_m^k \end{bmatrix} \approx \alpha_1^k \begin{bmatrix} \phi_1^1 \\ \phi_2^1 \\ \vdots \\ \phi_{m-1}^1 \\ \phi_m^1 \end{bmatrix} + \alpha_2^k \begin{bmatrix} \phi_1^2 \\ \phi_2^2 \\ \vdots \\ \phi_{m-1}^2 \\ \phi_m^2 \end{bmatrix} + \cdots + \alpha_m^k \begin{bmatrix} \phi_1^r \\ \phi_2^r \\ \vdots \\ \phi_{m-1}^r \\ \phi_m^r \end{bmatrix} \qquad \text{Equation 2-12}$$

Equivalently, equation 2-12 could be expressed in scalar-vector notation as

$$\boldsymbol{u}^k = \alpha_1^k \boldsymbol{\Phi^1} + \alpha_2^k \boldsymbol{\Phi^2} + \cdots + \alpha_r^k \boldsymbol{\Phi^m} \qquad \text{Equation 2-13}$$

Where $\boldsymbol{\Phi}$ refers to **r** most dominant proper orthogonal modes of $\boldsymbol{\psi}$**.** What is more, the displacement filed described in equation 2-13 would correspond to a set of simulated parameters $\widehat{\theta}(\theta^1 < \hat{\theta} < \theta^m)$. Consequently, equation 2-13 could be rewritten as

$$\hat{\boldsymbol{u}} = \hat{\alpha}_1 \boldsymbol{\Phi^1} + \hat{\alpha}_2 \boldsymbol{\Phi^2} + \cdots + \hat{\alpha}_2 \boldsymbol{\Phi^r} \qquad \text{Equation 2-14}$$

Moreover, in order to compute coefficients $\hat{\alpha} = (\hat{\alpha}_1, \hat{\alpha}_2, \ldots, \hat{\alpha}_r)$ ORION then employs the MLS method. This interpolation technique interpolates solutions for coefficients in $\hat{\alpha}$ from the matrix α by means of the following expression

$$\hat{\alpha} = \alpha \mathbf{N} \qquad \text{Equation 2-15}$$

Where **N** would are the number of interpolants that could be derived from

$$\hat{\theta} = \Theta^T \mathbf{N} \qquad \text{Equation 2-16}$$

There are numerous interpolation techniques that could be used to compute values for the coefficients in $\hat{\alpha}$. The moving least squares method approximates $f(u)$ to f_i by solving numerous small linear systems instead of one large system. Next, a weighted least squares fit is computed and evaluated for individual points by means of the following equation (Neaken, 2004)

$$f(u) = f_u(u), min_{f_u \in \Pi_m^r} \sum_i \theta(\|u - u_i\|) \|f_u(u) - f_i\|^2 \qquad \text{Equation 2-17}$$

Finally the proper orthogonal modes project the interpolated solutions back to the global solution space. The advantage of this method is that it further reduces the complexity of the initial data set, while still maintaining the ability to decrease the simulation of the MATLAB-Based Levenberg-Marquardt algorithm. Hence, this variation of POD will be used to obtain optimal material parameter constants for numerical simulations that will be investigated throughout this research project.

2.5 Concluding remarks

In conclusion, it could be seen that the constitutive material law approach that would be used in this research project would be that of the phenomenological approach. This approach would compare user defined experimental results to computer simulated results in order to find optimal non-linear constitutive constants.

The phenomenological approach will be combined with a technique called inverse modelling, more specifically, the updating method of inverse modelling. The updating method of inverse modelling aims to update a weighted multi-objective cost function which would be used to calibrate non-linear constitutive laws and consequently obtain optimal material constants.

To minimize the abovementioned multi-objective cost function Coleman et al. (1999), Essack (2014), Kanzow & Petra (2005), and The MathWorks (2015) all come to the same conclusion. A least squares method called the Levenberg-Marquardt Algorithm should be implemented to provide optimal results.

The primary drawbacks of Levenberg-Marquardt Algorithm is that as the complexity of the input parameters increase, so does the simulation time for output of results. For this, the MATLAB-based Levenberg-Marquardt Algorithm will be coupled with in-house POD-based software ORION to overcome this hindrance. From this standpoint, rendering simulated results will obtained and compared to experimental results.

3. Computational mechanics

3.1 Introduction

In recent years the importance of the continuum concept in engineering work has become more pronounced. This concept is based on the assumption that all matter is continuous, however it is known that for varying scales of material mechanics this statement is not true. Using a titanium specimen as an example, modelling this material body as a continuous specimen would make it easier to compute constitutive behaviour of said specimen. However, if the same specimen is observed on an even smaller scale, the nano mechanics scale for example, it is evident that the specimen in question consists of atoms. On an even smaller scale, it could be seen that these atoms consist of a core of protons and neutrons orbited by electrons (Mase & Mase, 1999). Consequently cementing the claim that material bodies are not entirely continuous. Computational mechanics is based on the assumption that all elements of which a material specimen is comprised of, behave in the same manner. Additionally it makes use of mathematic operators such as scalars, vectors, and Cartesian tensors to analyse the kinematic and mechanical behaviour of materials modelled on the continuum assumption.

Section 2 gave the reader a preliminary review of one of the considerations taken into account for modelling the above mentioned concept. Firstly, this chapter outlines an important concept of computational mechanics, namely, the balance law of continuum mechanics. Secondly, this section provides a general derivation of the stress exerted on a deformable material body. Thirdly, this section provides an outline of stress measures important to this work, namely the second Piola-Kirchoff stress tensor. Finally, this section concludes by providing the reader with sufficient description on how the virtual work and its discretization are coupled.

3.2 Balance law of continuum mechanics

From the above mentioned description of the computational concept it follows that this concept should have balancing laws. Mase & Mase (1999) explains that if a material body is subject to any kind of load, temperature change, or pressure change, the following balancing laws should be adhered to:

- **The law of conservation of mass:** this law ensures that there is no mass lost or gained when a material body deforms under applied loads.
- **The law of linear and angular momentum conservation:** this law defines the change in linear and angular momentum much like Newton's second law of motion in that the rate of change in linear and angular momentum over time, results in force and momentum
- **The law of energy conservation:** this law is related to the principle law of energy, stating that energy can neither be created or destroyed but that it could only be transferred from one medium to another

3.3 Kinematics in three dimensional Euclidean coordinates

According to Haupt (2000), kinematics is a branch of physics that describes the geometry of motion and deformation of a material body. Consider figure 3-1, which exhibits an arbitrary

material body **ß**, situated in a three dimensional Euclidean space **E**. As with most engineering tasks involving computation of a deformed material body, it would be simpler to compute the motion and deformation of a material body when said body has a reference configuration. The current (deformed) configuration could be compared to the reference configuration for an accurate representation motion and deformation.

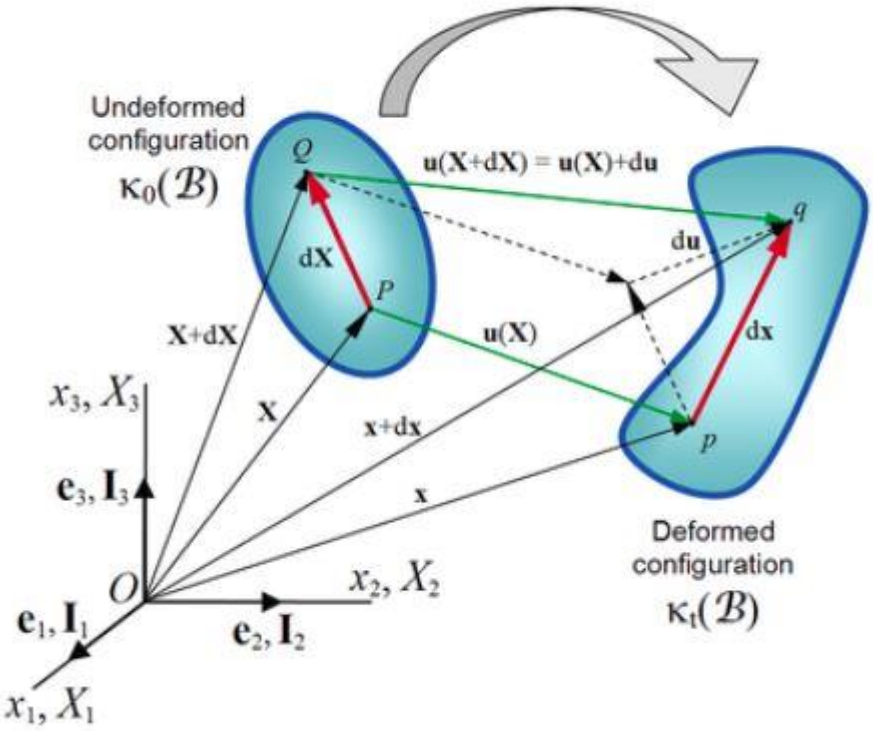

Figure 3-1: Kinematic deformation of a material body (Hopkins, 2014)

In this work, the author is investigating the constitutive behaviour of material specimens subject to a uniaxial tensile load. It could be said that the motion and deformation category of kinematics should be investigated. For a more detailed description of this physical phenomena, the following information has been outlined by Essack (2014) and Hopkins (2014) but the reader may find detailed descriptions of equations in Oden (2008), Mase & Mase (1999), and Sansour & Kollman (1997):

First let us consider the current configuration for the material body **ß** in a similar space as mentioned before. In this space, **E**, **ß** could be parametrized by the Cartesian coordinates X_1, X_2, and X_3 with their respective basis vectors $\mathbf{e}_1$, $\mathbf{e}_2$, and $\mathbf{e}_3$ respectively. To investigate the motion and deformation of **ß**, one needs to look at the duration of deformation and direction in which deformation takes place

In order to describe the movement of a particle from the reference configuration to the deformed configuration, a second order tensor referred to as the deformation gradient could be utilised. This deformation gradient characterizes the transformation of any point in **ß** with respect to time and could be expressed as

$$\boldsymbol{F} = \boldsymbol{F}_j^i\left(\boldsymbol{e}_i \otimes \boldsymbol{I}^j\right)$$

$$= \frac{\partial x^i}{\partial X^j} \otimes \boldsymbol{I}^j \qquad \text{Equation 3-1}$$

Where ∂X and ∂x refer to the material line elements in the reference and deformed configurations respectively. Consequently, if the transformation of a point within **ß** could be mathematically mapped it follows that the overall deformation of the material body **ß** could be obtained as well Hopkins (2014).

As described in the section 2.3.2, a rubber specimen exhibits highly non-linear behaviour when subject to uniaxial tensile loads while a titanium specimen would exhibit elastic behaviour until it reaches a yielding point after which it starts to exhibit plastic behaviour. Even though the former material would exhibit highly non-linear constitutive behaviour, it should be noted that rubbery materials behave elastically until it reaches its fracture point. In contrast, the latter material would exhibit elastic deformation up to a certain point, also referred to as the materials yield point, after which it would begin to exhibit plastic behaviour.

According to Sansour & Kollman (1997) a material that may exhibit elastic or plastic constitutive behaviour could be assumed to be dependent on a logarithmic strain measure which in the context of this work would be the Cauchy-Green strain measure. Consequently, it would be convenient to introduce the Cauchy-Green deformation vector as

$$\boldsymbol{C} = \boldsymbol{F}^T\boldsymbol{F} \qquad \text{Equation 3-2}$$

In the event that a material exhibits elastic constitutive behaviour the right Cauchy-Green strain measure could be written as

$$\boldsymbol{C}_e = \boldsymbol{F}_e^T\boldsymbol{F}_e \qquad \text{Equation 3-3}$$

Where the subscript **e** denotes elasticity, while the superscript **T** denotes the transpose operator. Additionally, if a material were to display plastic constitutive behaviour the right Cauchy-Green strain measure could be written as

$$\boldsymbol{C}_p = \boldsymbol{F}_p^T\boldsymbol{F}_p \qquad \text{Equation 3-4}$$

Where the subscript **p** denotes plasticity. In this work, the author investigates the constitutive behaviour of a titanium specimen subject to uniaxial tensile loads which is known to display elastic and plastic deformation respectively before failure of the specimen occurs. In the event that a material displays this sort of behaviour, Sansour & Kollman (1997) outlines a method of taking both instances into account by expressing the final deformation gradient by means of

multiplicative decomposition as

$$\boldsymbol{F} = \boldsymbol{F}_e \boldsymbol{F}_p \qquad \text{Equation 3-5}$$

The abovementioned equations would serve as a precursor to constructing constitutive modelling equations in section 4.

3.4 Stress measures

In order to understand the effect of stress measures and how they will be utilised in this work let us consider a deformable body in a three dimensional space, refer to figure 3-2 subjected to arbitrary loads to form an equilibrium condition. It could be said that at any point within this body has Cartesian vectors $\mathbf{X}_1$, $\mathbf{X}_2$, and $\mathbf{X}_3$.

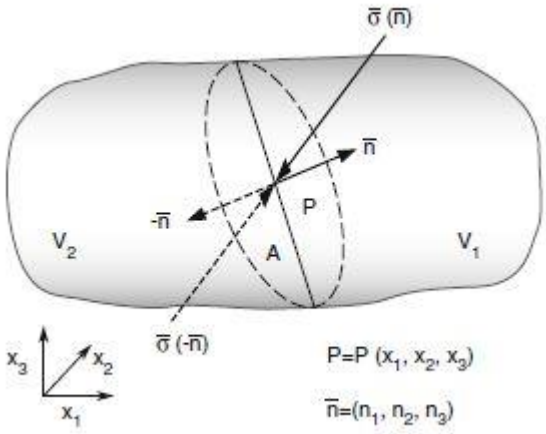

Figure 3-2: Deformable material body (Zang & Stephansson, 2010)

At point **P**(x) let us imagine a plane **A** slicing through the deformable material body at an angle with unit vectors $\mathbf{e}_1$, $\mathbf{e}_2$, and $\mathbf{e}_3$.This plane, **A**, divides the deformable body into two volumes namely V_1 and V_2, both of which have normal vectors –**n**(x) and +**n**(x) respectively. Consequently, it could be said that V_1 exerts a force on V_2, let's call this force **F**(x). Moreover, engineering stress could be computed as the ratio of force to the undeformed surface area of an arbitrary solid body. In the same manner the stress vector could be defined as the ratio of the resultant force **F**(x) to the area **A**. (Zang & Stephansson, 2010)

Now that the reader has a basic understanding of stress measures, the author introduces a stress measure that will be used for this work. In order to compute large deformations, more applicable measures of defining stress are required. For this, the second Piola-Kirchoff tensor could be used to compute large deformations. This stress tensor could be used to measure the transformation of forces per unit area from the reference configuration to the current configuration and could be written as (Batra, 1998)

$$\boldsymbol{S} = J\boldsymbol{F}^{-1}\boldsymbol{\sigma}\boldsymbol{F}^{-T}$$

$$= \boldsymbol{C}^{-1}\boldsymbol{\Xi} \qquad \text{Equation 3-6}$$

Where **F** is the aforementioned deformation gradient, **J** is the Jacobian determinant of the deformation gradient, and σ refers to the Cauchy stress tensor. From this standpoint, the author notes that the second Piola-Kirchoff stress tensor would be used to construct a constitutive model for elastic constitutive behaviour described in section 4.4.2.

3.5 Finite element method

As outlined in section 1.1.2, the importance of using extremely powerful numerical methods have become more apparent in recent years. One such numerical method could be described as the finite element method, which could be used to analyse linear and non-linear numerical problems.

The definition of the finite element method, as the name of the method suggests, is that it discretizes the structure of interest into a finite number of elements. By using the method of discretization, the finite element method separates the structure of interest into a finite set of subdomains. (de Weck & Yong Kim, 2004)

Next, unknown variables are approximated for individual subdomains. These variables could include stress, strain, pressure, and force per unit length. The approximation of unknown variables is done by a linear combination of algebraic polynomials and undetermined parameters (Reddy, 2015). Such that the algebraic relations among the unknown parameters could be obtained by satisfying a global equation system which could be in the form of

$$\boldsymbol{K}u = \overline{\boldsymbol{F}} \qquad \text{Equation 3-7}$$

Where u refers to the displacement matrix of nodes that reconnect individual finite elements and $\overline{\boldsymbol{F}}$ denotes the global force matrix made up of forces applied to each node. Furthermore, K refers to the global stiffness matrix made up of nodal stiffness coefficients. It should be noted that nodal stiffness coefficients take into account the elasticity, area, and length of a finite element. Finally, the overall process results in a set of simultaneous algebraic equations that could either be analysed by in-house mesh free software such as SESKA or by the finite element software package itself using equilibrium considerations. (de Weck & Yong Kim, 2004)

3.6 Principle of virtual work and its discretization

In every structural system there are numerous forces present, whether it be internal or external, to which a certain capacity could be associated. This capacity could be described in terms of a capacity to displace and to do work, respectively (Oden & Ripperger, 1981).The aforementioned capacity could also be categorized as a broader description of energy principles. One such energy principle that was found to be important is that of virtual work.

The general principle of virtual could be defined in terms of a single particle at the material level in terms of Newton's second law. That is, if a particle is at equilibrium under the action of

a number of forces (external and internal) then the total work done by the forces (internal and external) for virtual work should equate to zero. For the purpose of this work, the author notes that virtual work could be seen as the most effective analysis tool with regard to defining the relation between the displacements caused by various forces acting on a structural system. What follows is two major advantages of the virtual work method as outlined by Reddy (2015):

- The virtual work method is useful in determining the position of equilibrium in a structural system where the external loads are known, and
- The virtual work method neglects the effects of internal frictional forces

From the advantages described above it could be seen that the virtual work method could be implemented manually, depending on the problem being investigated. Recently, this method has been coupled with various structural analysis and finite element software where it could be used to analyse more complex problems. Using the finite element analysis software described in section 1.1.2, material elements could be discretized into a finite number of elements from the structural level to the material point level. Computations are carried out at the material point level and then assembled at the structural level. According to Reddy (2015) the finite element model could be formulated using the principle of virtual work as

$$\text{Internal work done} - \text{External work done} = 0 \qquad \text{Equation 3-8}$$

Where internal work done refers to extensional, extensional-bending coupling, and bending fourth-order stiffness tensors. In contrast, the external work done takes into account external forces acting on the model being investigated. Thus, coupling finite element software with the method of virtual work would allow the user to overcome the effect of manual computation of moments, forces, and forces per unit length. Table 3-1 was adopted Reddy (2015) and generally displays the number of terms of virtual internal energy for different physical problems.

Table 3-1: Virtual strain energy variables

			Virtual strain energy		
Theory	Application	Kinematic variables	Linear	Non-linear	Total
Beam*	Moderate rotations	2	2	3	5
2D Navier-Stokes equations**	----	3	10	4	14
Beam*	Finite deformations	5	13	109	122
Cylindrical shells	Moderate rotations	5	106	193	299
Rectangular plates	Finite deformations	7	136	2,245	2,381
Circular plates	Finite deformations	7	232	5,197	5,429
Spherical plates	Finite deformations	7	666	19,630	20,296
Hyperboloid shells	Finite deformations	7	699	19,424	20,123
*Isotropic cases, **Newtonian fluid with constant viscosity					

3.7 Concluding remarks

In this section, an outline of the underlying theory used to describe the kinematics of a material body in three dimensional Cartesian space. Additionally, the provision of three balancing laws that computational mechanics need to obey to effectively model the mechanical behaviour of materials. Subsequently, this section gave the reader a basic mathematical understanding of the kinematic response of a material body. Furthermore, this section gave the reader a general description of stress measures and a type of stress measure that could be used for the purpose of this work. Moreover, this section concludes by providing the reader with a basic understanding of the finite element method, the principle of virtual work and its discretization.

4. Constitutive material law theory

4.1 Introduction

In section 2.3, the author introduced the concept of constitutive behaviour. Additionally in the aforementioned section, an outline of the constitutive behaviour of hyperelastic and elastoplastic materials could be found. The focus of this section is to provide an overview of traditional constitutive material theory which could be used for hyperelastic and elastoplastic materials, respectively. According to William (2002) constitutive models relate kinematic description of a material body in order to close the formulation of an initial boundary value problem. In the following section, the constitutive theory being discussed would be used to describe the mechanical behaviour of vulcanized rubber and titanium, respectively. Moreover, these constitutive material laws could broadly be used to investigate the life-cycle performance of civil, mechanical, and aeronautical structures.

The layout of this section is as follows, firstly it discusses the constitutive law theory of hyperelastic materials which would include a detailed description of the topic and generalised method of constructing a hyperelastic constitutive material law. Secondly, this section would include a detailed description of elastoplastic constitutive material law theory and the various methods if implementing these theories. Finally, this section would discuss how the author came to the concluding remarks on which constitutive materials law would be used for vulcanized rubber and titanium, respectively.

4.2 Hyperelastic constitutive law theory

Hyperelastic constitutive laws could be used to model the mechanical behaviour of materials that exhibit very large elastic strain before it fractures. It is important to note that when modelling the constitutive behaviour of hyperelastic materials, the load history is path independent and the temperature at which the experiment is conducted needs to be recorded.

Figure 4-1 exhibits a critical aspects to consider when modelling the mechanical behaviour of polymeric materials, namely temperature. From the aforementioned figure, it could be seen that at a critical temperature, known as the glass transition temperature, is where this material undergoes a dramatic change in mechanical behaviour response. Moreover, as the temperature of experimental conditions increases the mechanical behaviour of this material would exhibit further changes in constitutive behaviour. The temperature at which this secondary change in constitutive behaviour occurs is known as the crystallisation melting point temperature. (University, 2015)

With regard to constitutive behaviour, before a polymeric material reaches its glass transition temperature it exhibits a stiff constitutive response, much like glass. Moreover, once the material surpasses its glass transition temperature it experiences a drop in elasticity until it reaches its crystallisation melting point. Once the polymeric material exceeds its crystallisation melting point temperature, the regime of this material exhibits a rubber-like behaviour. Contrary to the region in which said material would exhibit glassy behaviour, in the region of rubber-like behaviour the stress does not depend on the strain rate of strain history. Hyperelastic constitutive laws are intended to predict the mechanical response polymeric materials that surpass its

crystallisation melting point temperature.

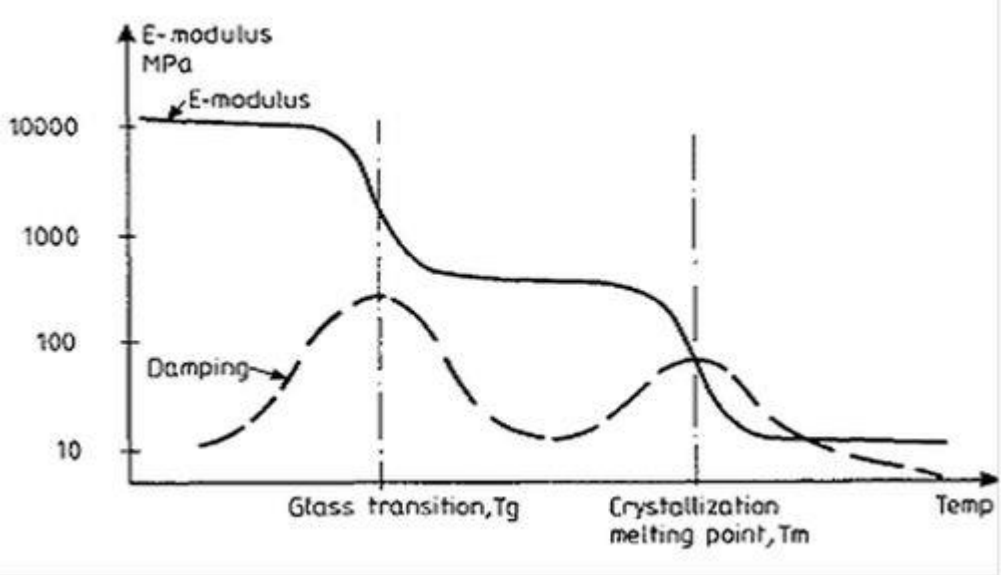

Figure 4-1: Shear modulus vs temperature (Nexans, 2009)

In order to model the constitutive behaviour of hyperelastic materials, the appropriate research was done to understand the typical behaviour of rubber-like materials and what one needs to consider when constructing a constitutive model to approximate the constitutive behaviour of hyperelastic materials. In light of this, Bower (2009), William (2002), and Kim (2015) outline the aforementioned needs of the author. The typical features of features of a rubber-like material, as described by Bower (2009), are as follows

- The material is to be modelled as an ideally elastic material, meaning that under constant temperature the stress induced by elongation is a function of current strain and not on the rate of loading.
- The material should be modelled as if it could strongly resist volume changes.
- The material is compliant in shear, meaning that the value of shear modulus is small.
- The constitutive response of this material is independent of the material configuration.
- The shear modulus of this material is temperature dependant, as described in figure 4-1.
- The material gives off heat when subject to large strains.

From the abovementioned behavioural traits, it could be seen that all hyperelastic models could be constructed using a systematic procedure. In order to construct a hyperelastic constitutive material model, Kim (2015) discusses three basic procedures that could be used to predict the mechanical behaviour of hyperelastic materials, these are

- Defining a constitutive relationship for a material body by specifying its strain density, **W**, as a function of a material specific deformation gradient described in equation 3-1. It should be noted that **W** should always contain material properties that could define the material body in question.
- The undeformed configuration, also referred to as the reference configuration, is usually assumed to be isotropic where the strain density function would make use of the

Cauchy-Green stress tensor described in equation 3-3. With regard to relating stress and strain to one another, it should be noted that the strain density of a material body should be expressed in terms of invariants of the deformation measure of the left Cauchy-Green deformation measure.

- Formulas for stress in terms of strain could then be calculated by differentiating strain energy density equations, which would vary depending on a user-defined material law.

4.3 Hyperelastic material models

For the provision of a better understanding of the various material laws that could be categorized as hyperelastic, the author needs to describe the primary differences in these material laws, that being the difference in strain energy density functions. As a preamble to the aforementioned function, the reader needs to have a basic understanding of deformation measures and stress measures associated to hyperelastic material models. It should be noted that the methods proposed in this section was adopted form Kim (2015) and William (2002), and was not developed by the author.

In general, the strain energy density function could be described in terms of a material body's strain invariants $\boldsymbol{I}$ of the right Cauchy-Green stress tensor **C** described in equation 3-3 and could be expressed as

$$\boldsymbol{I}_1 = \mathrm{tr}\mathbf{C} = \lambda_1^2 + \lambda_2^2 + \lambda_3^2 \qquad \text{Equation 4-1}$$

$$\boldsymbol{I}_2 = \frac{1}{2}[(\boldsymbol{C}^T)^2 - (\boldsymbol{C}^2)^T]$$

$$= \lambda_1^2\lambda_2^2 + \lambda_2^2\lambda_3^2 + \lambda_3^2\lambda_1^2 \qquad \text{Equation 4-2}$$

$$\boldsymbol{I}_3 = detC = \lambda_1^2\lambda_2^2\lambda_3^2 \qquad \text{Equation 4-3}$$

Where tr**C** and det**C** is the trace and determinant of the right Cauchy-Green deformation tensor **C,** respectively while λ_1^2, λ_2^2, λ_3^2 represent the Eigen values of the left Cauchy-Green deformation tensor **C**. Using the invariants described in equations 4-1, 4-2, and 4-3 Kim (2015) formulates a general equation from which the strain energy density can be defined from and could be written as follows

$$W(\boldsymbol{I_1}, \boldsymbol{I_2}, \boldsymbol{I_3}) = \sum_{m+n+k=1}^{\infty} A_{mnk}(\boldsymbol{I}_1 - 3)^m(\boldsymbol{I}_2 - 3)^n(\boldsymbol{I}_3 - 1)^k \qquad \text{Equation 4-4}$$

Where A_{mnk} are coefficients of polynomials. Additionally, Bigoni (2012) outlines how the various hyperelastic constitutive models could be formulated using variations of equation 4-4 depending on the accuracy required by the user. Moreover, it was noted that the accuracy of hyperelastic constitutive models outlined in literature increases as their polynomial order

increases. From this, the author notes that the simplest approach to modelling the constitutive behaviour of hyperelastic material is that of the Neo-Hookean approach.

In general, using the Neo-Hookean approach to model an incompressible isotropic material, the strain density function only has one nonzero parameter A_{10} while all other parameters are set to zero. Using the reference configuration, the aforementioned function could be defined as

$$W_1(\boldsymbol{I}_1) = A_{10}(\boldsymbol{I}_1 - 3) \qquad \text{Equation 4-5}$$

Furthermore, for the purpose of this research project equation 4-5 has been updated by making use of the St. Venant-Kirchhoff non-linear elastic strain energy density function which could be defined as

$$\begin{aligned} W(\boldsymbol{E}) = & \ \frac{1}{2}\boldsymbol{E}:\boldsymbol{D}:\boldsymbol{E} \\ = & \ \frac{1}{2}E:\lambda\boldsymbol{I}\otimes\boldsymbol{I} + 2\mu\boldsymbol{I}:E \end{aligned} \qquad \text{Equation 4-6}$$

Where **E** is strain, **D** as the fourth-order constitutive tensor for isotropic materials, and '**:**' could be defined as the contraction operator of tensors. From equation 4-6, λ and μ are Lamé parameters for isotropic materials and could be expressed as

$$\lambda = \frac{\nu E}{(1+\nu)(1+2\nu)} \qquad \text{Equation 4-7}$$

$$\mu = \frac{E}{2(1+\nu)} \qquad \text{Equation 4-8}$$

Here, E refers to Young's modulus and ν is poisons ratio. Equations 4-7 and 4-8 could easily be used to calibrate a material specimen in virtual environment, for example GiD, such that a comparison between simulated and experimental data would provide small deviations in constitutive values.

4.4 Elastoplastic constitutive law theory

4.4.1 Small strain theory

The underlying theory of elastoplastic constitutive material models could be constructed from several points of departure. In general, William (2002) proposes that an optimal point of departure to predict elastoplastic behaviour would be an assumption that the stress tensor may be represented as a function of the current strain tensor and a finite number of parameters which could be expressed as

$$\boldsymbol{\sigma} = f(\varepsilon, q_1, q_2, \ldots\ldots, q_n) \qquad \text{Equation 4-9}$$

For the purpose of this work, the elastoplastic rheological spring and friction element subject to uniaxial conditions could be used to develop constitutive relations. The key aspects of the aforementioned element are displayed in figure 4-2; where E represents Young's modulus, σ_y (ε_p) denotes plastic strain at yielding while σ denotes engineering stress and 1+ε refers to the stretch ratio

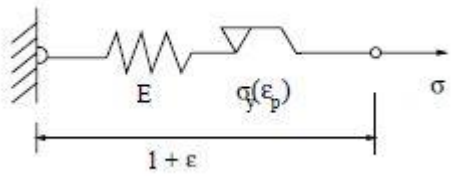

Figure 4-2: elastoplastic rheological spring and friction element (William, 2002)

In small deformation theory it is proposed that the overall strain of a material specimen is the additive decomposition of elastic and plastic strain-energy components which could be defined as

$$\varepsilon = \varepsilon_e + \varepsilon_p \qquad \text{Equation 4-10}$$

Where subscripts e and p denote elastic and plastic strain regimes, respectively. The relationship described in equation 4-10 provides a distinct difference between the non-linear material described in section 2.3 and an elastoplastic material. The elastic strain occurs within the linear elastic regime, here the strain response of an elastoplastic material specimen could be described as

$$\varepsilon_e = \frac{\boldsymbol{\sigma}}{E} \qquad \text{Equation 4-11}$$

It is important to note that this formula applies to the regime where the stress induced in a material is less than said materials yield stress. With reference to equation 4-10, it could be seen that the total strain exhibited by a material would change as the plastic strain changed. In general, plastic strain accumulates when a material exceeds its yield strength thus it is imperative that every load increment should be known in order to calculate the effective plastic strain at a certain time increment (Sansour & Kollman, 1997). Moreover, the load history of a material specimen should be known in order to compute the overall stress within said material specimen. Consequently, equation 4-11 could be manipulated to display the overall plastic strain response of a material and could be described as

$$\varepsilon_p = \frac{\boldsymbol{\sigma}}{E_p} \qquad \text{Equation 4-12}$$

Where E_p could be referred to as the plastic modulus and could further be defined as the slope of the strain-hardening part of the stress-strain curve. Substituting equations 4-11 and 4-12 into equation 4-10 the author arrives as

$$\varepsilon = \frac{\boldsymbol{\sigma}}{E} + \frac{\boldsymbol{\sigma}}{E_p} = \frac{\boldsymbol{\sigma}}{E_{ep}}$$ Equation 4-13

Where E_{ep} denotes the elastoplastic tangent stiffness. Figure 4-3, graphically describes the constitutive response to cyclic loading.

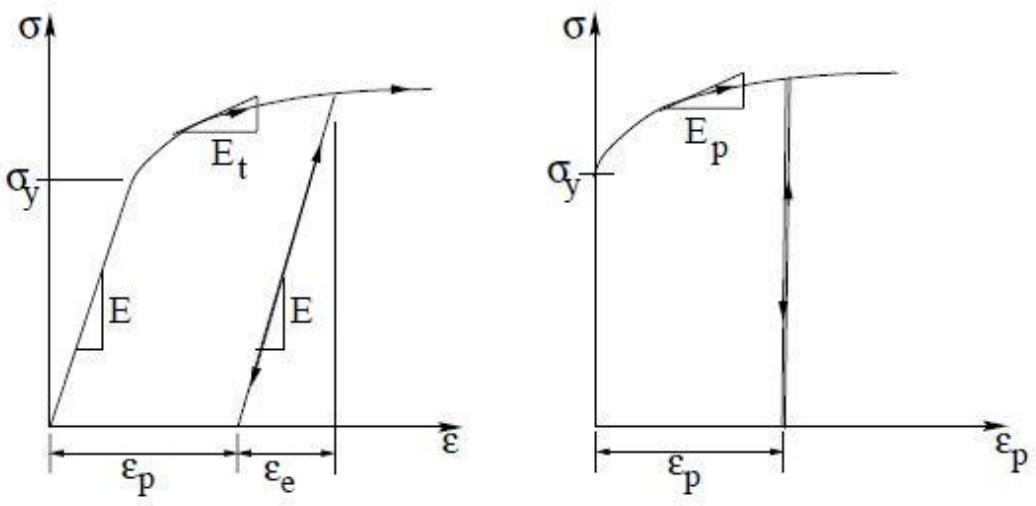

Figure 4-3: Constitutive relationship of a ductile metal (William, 2002)

In order to construct a constitutive model to accurately predict the mechanical behaviour of an elastoplastic material, the general constitutive flow of said material needs to be taken into consideration. Subsequently, using figure 4-3 as a point of reference, Neto et al. (2008) outlines the general aspects of an elastoplastic constitutive model take into account the following aspects

- The elastic behaviour of the specimen, which starts at the free energy function
- The plastic yield condition of the specimen, which could be explained as a condition that relates the hardening modulus to yield resistance of the specimen
- The plastic flow rule, which denotes the evolution of plastic strain
- The plastic consistency condition, which forces the stress path of the material to remain on the yield surface
- The elastoplastic stiffness relation, which could be used to relate the stress and strain rates

There are numerous yield criterions that could be used to determine whether a material has yielded or not. Moreover, for the purpose of engineering materials, the Tresca and von Mises yield criterion is commonly used for this specific purpose. In the following section, the author will compare the classical yield criterions proposed Henri Tresca and Richard von Mises. It should be noted that the methods proposed in this section were adopted form Neto et al. (2008), Bower (2009), Sansour & Kollman (1997), and was not developed by the author.

The Tresca criterion, named after its discoverer Henri Edouard Tresca, describes the maximum shear stress criterion of material failure. In 1864 Henri Edouard Tresca conducted a series of experiments investigating plastic flow of materials, subject to various tensile loads, at large stresses during tensile testing (Rice, 2010). Upon investigating the plastic flow of ductile materials, Tresca discovered that a material would flow plastically if σ_1 less σ_3 is greater than the maximum shear stress that a material could withstand before yielding. Where σ_1 could be defined as the the maximum principal stress direction, σ_2 the intermediate principle stress direction, and σ_3 the minimum principle stress direction. Consequently, Tresca's yield criterion could be defined as

$$\frac{1}{2}(\sigma_1 - \sigma_3) = \tau_y(\alpha) \qquad \text{Equation 4-14}$$

Where τ_y is the shear stress and α denotes internal hardening variable of said material specimen. According to Neto et al. (2008), the stress level at which yielding occurs begins under uniaxial stress conditions thus, the author notes that for a material specimen subject to uniaxial tensile loads the principal stresses mentioned in equation 4.14 could be described as

$$\sigma_1 = \sigma_y \qquad \text{Equation 4-15}$$

$$\sigma_3 = 0 \qquad \text{Equation 4-16}$$

Where $\boldsymbol{\sigma}_y = 2\tau_y$, denotes yield stress. Consequently, substituting equations 4-15 and 4-16 into equation 4-14 Tresca's yield function could be defined as

$$\Phi(\sigma) = \sigma_y - \sigma_y(\alpha) \qquad \text{Equation 4-17}$$

In general, an important aspect of defining yield criterion is that of isotropy. Isotropy, also shared by the von Mises yield criterion, is defined as the property of a material that would exhibit an identical mechanical response independent of the chosen direction of the material element Hashiguchi (2009). Figure 4-4 displays an isotropic material body that would exhibit similar material properties independent of the applied force/s.

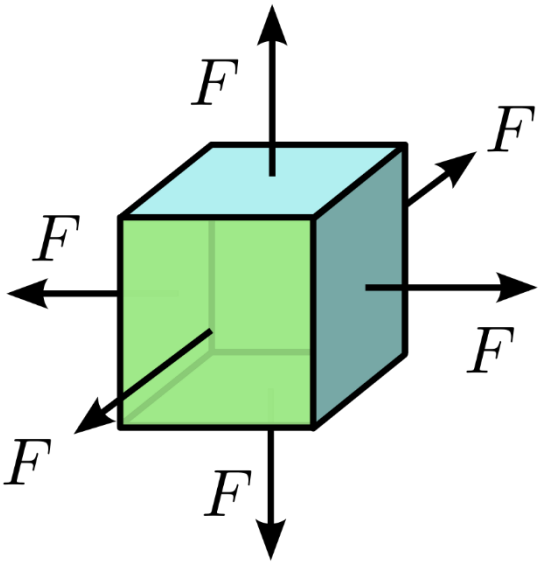

Figure 4-4: Isotropic material (Stolfi, 2013)

In addition to material isotropy, Neto et al. (2008) notes that the effect of pressure sensitivity could be relevant in the modelling of elastoplastic materials. Moreover, it was brought forward that the influence of pressure sensitivity, also known as the hydrostatic pressure component, is usually neglected in practise. From this stand point, the author notes that pressure sensitivity should be taken into account in order to provide an accurate yield criterion function.

In contrast to Tresca's yield criterion, Andriyana (2008) states that the basis of the von Mises criterion, named after its discoverer Richard von Mises, arises from the distortion energy theory. Consequently, the von Mises yield criterion proposes that plastic yielding begins when J_2 stress deviator invariant reaches a critical value. Moreover, he states that yielding occurs when the distortion energy component of a given material is equal to its maximum distortion energy and is described as

$$\boldsymbol{W}_{d,max} = \boldsymbol{W}_{d,y} \qquad \text{Equation 4-18}$$

Where $W_{d,max}$ denotes the maximum distortion energy and $W_{d,y}$ refers to the distortion energy component at yielding. Since the J_2 stress deviator invariant is the only influence on plastic yielding, pure shear stress and the second Piola-Kirchoff stress tensor could be defined as

$$[\boldsymbol{\sigma}] = [\boldsymbol{S}] = \begin{bmatrix} 0 & \tau & 0 \\ \tau & 0 & 0 \\ 0 & 0 & 0 \end{bmatrix} \qquad \text{Equation 4-19}$$

Where the J_2 stress deviator invariant could be expressed as

$$\boldsymbol{J}_2 = \tau^2 \qquad \text{Equation 4-20}$$

Thus the general von Mises yield function could be expressed as

$$\Phi(\boldsymbol{\sigma}) = \sqrt{\boldsymbol{J}_2(\boldsymbol{S}(\boldsymbol{\sigma}))} - \tau_y \qquad \text{Equation 4-21}$$

For the purpose of this work, the author notes that the use of a variation of equation 4-21 needs to be established in order to predict the constitutive behaviour of a material specimen subject to uniaxial loading. Neto et al. (2008) defines a variation in the shear stress and the second Piola-Kirchoff stress tensor as

$$[\boldsymbol{\sigma}] = \begin{bmatrix} \sigma & 0 & 0 \\ 0 & 0 & 0 \\ 0 & 0 & 0 \end{bmatrix} \qquad \text{Equation 4-22}$$

and

$$[\boldsymbol{S}] = \begin{bmatrix} \frac{2}{3}\sigma & \tau & 0 \\ \tau & -\frac{1}{3}\sigma & 0 \\ 0 & 0 & -\frac{1}{3}\sigma \end{bmatrix} \qquad \text{Equation 4-23}$$

Therefore the J_2 stress deviator invariant could be expressed as

$$\boldsymbol{J}_2 = \tfrac{1}{3}\boldsymbol{\sigma}^2 \qquad \text{Equation 4-24}$$

Consequently, an alternative to equation 4-21 could be defined as

$$\Phi(\boldsymbol{\sigma}) = \sqrt{3\boldsymbol{J}_2(\boldsymbol{S}(\boldsymbol{\sigma}))} - \boldsymbol{\sigma}_y \qquad \text{Equation 4-25}$$

Subsequently, from the aforementioned expressions it could be seen that the von Mises yield criterion would predict a yield stress $\frac{2}{\sqrt{3}}$ times greater than the Tresca yield criterion.

4.4.2 Finite strain theory

In section 4.4.1 the author presents that elastoplastic materials would be subject to two forms of strain, namely elastic and plastic strain. Moreover it was proposed by William (2002) that the extent of elastic strain induced in a material would have an effect on the total plastic strain present in said material specimen. For this reason, the author proposes the separate formulation of an elastic and plastic constitutive model, respectively. It should be noted that the methods proposed in this section was adopted form Neto et al. (2008), Bower (2009), Sansour & Kollman (1997), and was not developed by the author.

4.4.2.1 Elastic constitutive models

In order to construct an elastic constitutive model, a general elastic material stress tensor $\boldsymbol{\Xi}$ needs to be established, Sansour & Kollman (1997) expresses $\boldsymbol{\Xi}$ as

$$\boldsymbol{\Xi} = 2_{\rho_{ref}} \boldsymbol{F}_p^T \boldsymbol{C}_e \frac{\partial \psi(\boldsymbol{C}_e, \boldsymbol{Z})}{\partial \boldsymbol{C}_e} \boldsymbol{F}_p^{-T} \qquad \text{Equation 4-26}$$

Where ρ_{ref} denotes the density of the reference configuration as described in section 3.4, while $\boldsymbol{F}_\mathbf{p}$ refers to the deformation gradient tensor described in the aforementioned section. Moreover, ψ is the free energy function, while $\boldsymbol{C}_e$ refers to the elastic part of the right Cauchy-Green and $\boldsymbol{Z}$ refers to the phenomenological internal variable such that $\psi(\boldsymbol{C}_e, \boldsymbol{Z})$.

During the elastic constitutive regime the free energy variable ψ could be expressed with respect to $\boldsymbol{C}_e$ and $\boldsymbol{Z}$ such that

$$\psi = \psi_e(\boldsymbol{C}_e) + \psi_Z(\boldsymbol{Z}) \qquad \text{Equation 4-27}$$

For convenience, the natural logarithmic strain measure $\boldsymbol{\alpha}$ could be introduced and would be expressed as

$$\boldsymbol{\alpha} = \ln(\boldsymbol{C}_e) \qquad \text{Equation 4-28}$$

Consequently, from the above expressions, Sansour & Kollman (1997) discovered that for an isotropic elastoplastic material in the elastic regime the following expression holds true

$$\boldsymbol{C}_e \frac{\partial \psi(\boldsymbol{C}_e, \boldsymbol{Z})}{\partial \boldsymbol{C}_e} = \frac{\partial \psi(\boldsymbol{\alpha})}{\partial \boldsymbol{\alpha}} \qquad \text{Equation 4-29}$$

Subsequently, equation 4-26 could alternatively be expressed in terms of the natural logarithmic strain measure as

$$\boldsymbol{\Xi} = 2_{\rho_{ref}} \boldsymbol{F}_p^T \frac{\partial \psi(\boldsymbol{\alpha})}{\partial \boldsymbol{\alpha}} \boldsymbol{F}_p^{-T} \qquad \text{Equation 4-30}$$

In order to increase computational efficiency a simplified version of equation 4-16 needs to be constructed, consequently the natural logarithmic strain measure could be modified and expressed as

$$\bar{\boldsymbol{\alpha}} = \boldsymbol{F}_p^T \boldsymbol{\alpha} \boldsymbol{F}_p^{-1} \qquad \text{Equation 4-31}$$

To further increase computational efficiency, $\bar{\boldsymbol{\alpha}}$ could alternatively be expressed as

$$\bar{\boldsymbol{\alpha}} = \ln(\boldsymbol{C}_p^{-1} \boldsymbol{C}) \qquad \text{Equation 4-32}$$

or

$$\bar{\boldsymbol{\alpha}}^{\boldsymbol{T}} = \ln(\boldsymbol{C} \boldsymbol{C}_p^{-1}) \qquad \text{Equation 4-33}$$

Following the alternative version of the natural logarithmic strain measure introduced in equations 4-32 and 4-33, equation 4-26 could be further simplified and expressed as

$$\boldsymbol{\Xi} = 2_{\rho_{ref}} \frac{\partial \psi(\overline{\boldsymbol{\alpha}})}{\partial \overline{\boldsymbol{\alpha}}} \qquad \text{Equation 4-34}$$

Finally, for the purpose of this work, the author adopts an elastic constitutive model expressed as

$$\boldsymbol{\Xi} = \mathrm{K}\ \mathrm{tr}\overline{\boldsymbol{\alpha}}^{\boldsymbol{T}}\mathbf{1} + \mu\ dev\overline{\boldsymbol{\alpha}}^{\boldsymbol{T}} \qquad \text{Equation 4-35}$$

Such that K denotes bulk modulus and μ refers to the shear modulus of the specimen in question.

4.4.2.2 Plastic constitutive models

As described in section 4.4.4.1, as a material specimen surpasses its yield stress it would start to exhibit plastic behaviour. Moreover, since a graphical representation of the constitutive relationship of a ductile metal would produce a graph similar to Figure 4-3 the author notes that a plastic constitutive model needs to be constructed in order to identify optimal material constants. . It should be noted that the methods proposed in this section was adopted form Neto et al. (2008), Bower (2009), Sansour & Kollman (1997), and was not developed by the author.

Similar to the phenomenological internal variable $\boldsymbol{Z}$ proposed for the elastic constitutive model in section 4.4.2, a second internal variable $\boldsymbol{L_p}$ needs to be established to predict constitutive behaviour in the plastic regime. For this, Sansour & Kollman (1997), defines this variable $\boldsymbol{L_p}$ as the plastic rate of a material specimen. Moreover, it is required that the phenomenological internal variable $\boldsymbol{Z}$ and plastic rate $\boldsymbol{L_p}$ needs to be defined in terms of the yield function Φ since the regime change from elastic to plastic behaviour occurs at yielding. Furthermore, Sansour & Kollman (1997), assumes that the aforementioned statement is dependent on the thermodynamic quantities σ and Y such that

$$E \coloneqq \{(\boldsymbol{\Xi}, Y) \colon \Phi(\boldsymbol{\Xi}, Y) \leq 0\} \qquad \text{Equation 4-36}$$

Where the von Mises yield function could be expressed as

$$\Phi(\lambda, L_p) = \|dev\ \boldsymbol{\Xi}\| - \sqrt{\frac{2}{3}}\ (\sigma_y - Y\ ) \qquad \text{Equation 4-37}$$

Where $\|dev\ \boldsymbol{\Xi}\|$ denotes the norm of the tensorial quantity and σ_y refers to initial yield stress. Additionally, thermodynamic quantity Y could be expressed as a function of the material plastic multiplier λ as

$$Y(\lambda) = -H\left(Z_n + \sqrt{\frac{2}{3}}\,\Delta t\lambda\right) - (\sigma_\infty - \sigma_y)\left[1 - exp\left(-\eta\left(Z_n + \sqrt{\frac{2}{3}}\,\Delta t\lambda\right)\right)\right]$$

Equation 4-38

Since plastic strain is directly proportional to the elastic strain induced in a material specimen, Equation 4-38 is important with to understand the effect that plastic hardening has on a material specimen. Similar to Young's modulus E, *H* defines the plastic hardness modulus which controls the constitutive slope in the plastic regime. In addition to the plastic modulus *H*, η defines a second plastic material parameter which is inversely related to the plastic multiplier λ.

As expressed in section 4.4.3, the von Mises yield function Φ could be expressed in terms of three principle stress states σ_1, σ_2 and , σ_3. Figure 4-5 exhibits a graphical representation of the Tresca and von Mises yield criterion with respect to the aforementioned principle stress states. In general, for the inequality $\Phi < 0$ elastic deformation occurs which could be graphically represented as the function the function being inside the von Mises yield locus. Moreover, for the inequalities $\Phi = 0$ and $\lambda > 0$ said material specimen would be subject to plastic deformation which could be. Graphically represented as the function lies on the circumference of the von Mises yield locus. Consequently, for the inequality $\Phi > 0$ the von Mises yield function lies outside the yield locus which is not possible.

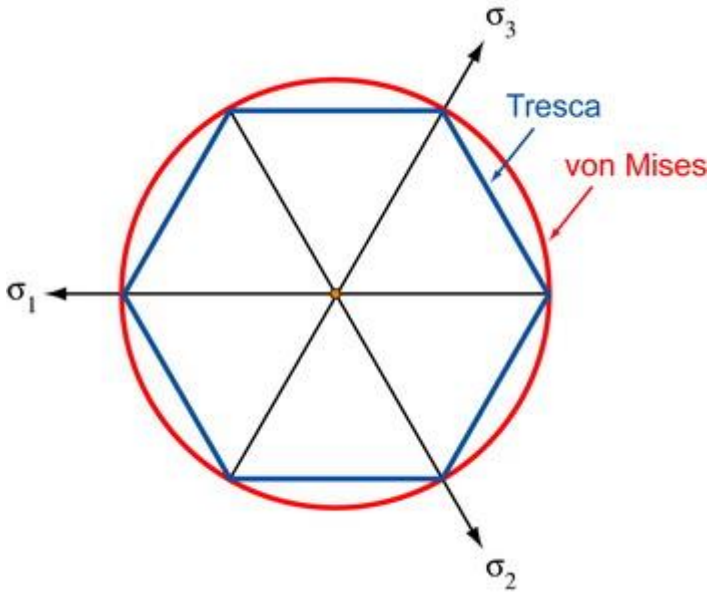

Figure 4-5: Graphical representation of the Tresca yield criterion and von Mises yield criterion (University of Cambridge, 2015)

.

In order to relate the plastic multiplier λ and the von Mises yield function Φ, the phenomenological internal variable $\boldsymbol{Z}$ and plastic rate $\boldsymbol{L_p}$ could be expressed as

$$\boldsymbol{L_p} = \lambda \frac{\partial \Phi}{\partial \boldsymbol{\Xi}}$$

$$= \lambda \frac{dev\ \boldsymbol{\Xi^T}}{\|dev\ \boldsymbol{\Xi}\|}$$

$$= \lambda \boldsymbol{v^T} \qquad \text{Equation 4-39}$$

$$Z = \lambda \frac{\partial \Phi}{\partial Y}$$

$$= \sqrt{\frac{2}{3}}\ \lambda \qquad \text{Equation 4-40}$$

4.5 Concluding remarks

Throughout this section the author describes the general considerations that need to be taken into account to construct hyperelastic and elastoplastic constitutive material laws. Moreover, at the end of this section the reader should have gained sufficient knowledge about hyperelastic and elastoplastic constitutive material models. Furthermore, this section further cements the fact that it would not be viable to use an analytical approach to compute the aforementioned constitutive material laws.

5. Numerical examples

5.1 Introduction

In sections 3 and 4, the author outlined the relevant theory of computational mechanics and constitutive material laws, respectively. From the knowledge gained throughout the research done for the aforementioned sections, and in order to complete the objectives outlined in section 1.3, the author analysed two types of materials. The core differences between these materials were the direction of the applied force, their respective geometric layouts, and material law proposed for each specimen.

5.2 Vulcanized rubber specimen

5.2.1 Experimental setup

With regard to non-linear behaviour of a hyperelastic material, the author analysed a natural rubber specimen subject to uniaxial deformation. Figure 5-1 displays the geometry of the specimen analysed by the author, this specimen was defined by a length of 10mm, a width of 3mm, and a thickness of 0.8mm. The proposed specimen has been modelled using 913 mesh free, as shown in table 5-1. In order to accurately simulate an experimental environment the author notes that the use of Dirichlet loading conditions to control deformation would not be feasible. Instead, it was noted that making use of Dirichlet boundary constraints would be a more accurate representation of an experimental environment. Consequently, the aforementioned specimen was subject to a displacement of 80mm. In addition, to avoid unwanted kinematic behaviour the author made use of symmetry and divided the specimen into two sections. Figures 5-2 and 5-3 illustrate how the author proposed to overcome problems associated with unwanted kinematic behaviour.

.

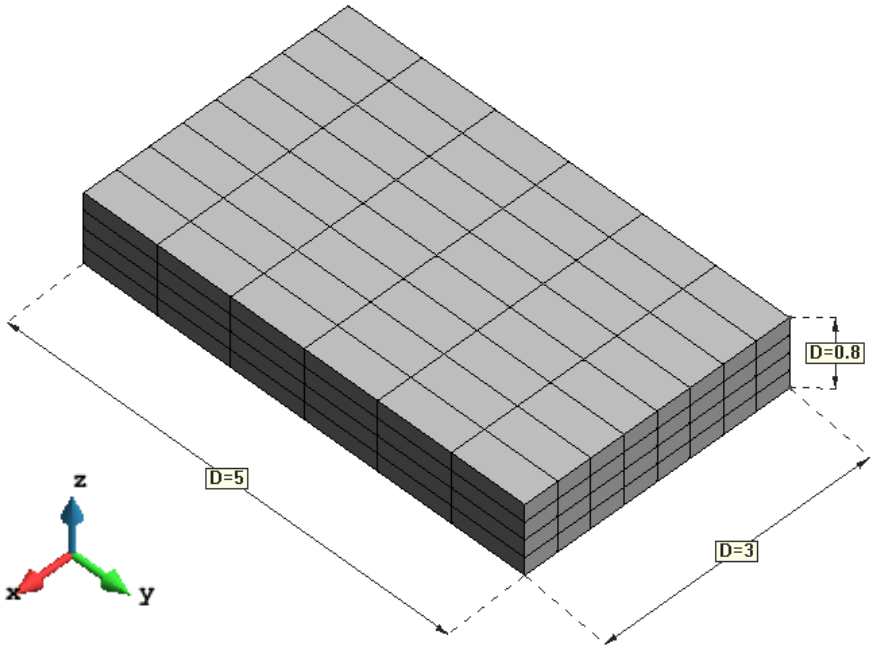

Figure 5-1: Geometry of material specimen

Table 5-1: Discretized materials meshed elements

Discretized materials meshed elements	
Element type	Number of elements
Linear elements	126
Quadrilateral elements	280
Hexahedra elements	192
Number of nodes	315
Total	913

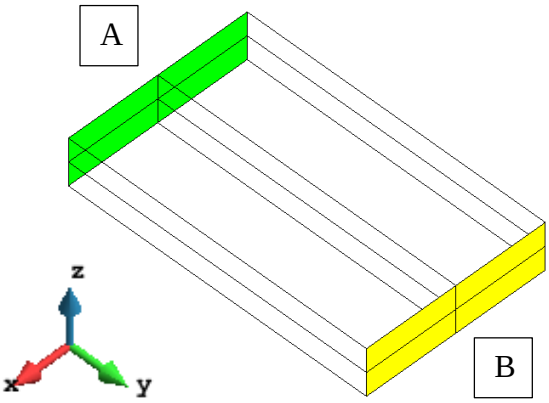

Figure 5-2: Dirichlet displacement surface-constraints

Considering Figure 5-2, the author applied a Dirichlet surface constraint at **A** with a value of zero in the direction of the applied Dirichlet boundary constraint such that no deformation of the surface to occur. Moreover, considering the same figure, the author applied a Dirichlet surface constraint at **B** such that an elongation of 80mm could be achieved.

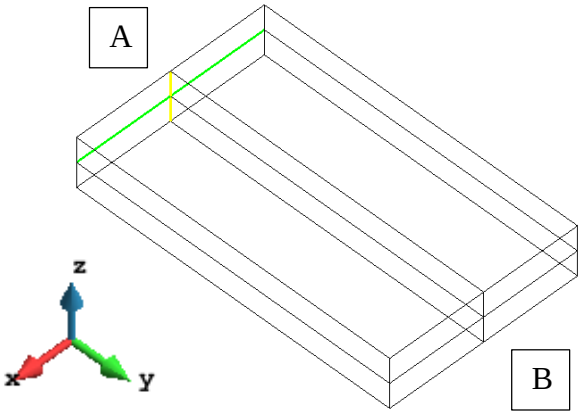

Figure 5-3: Dirichlet displacement line-constraints

With reference to figure 5-3, the green line refers to a line-constraint with a fixed deformation value of zero in the *z*-plane while the yellow line refers to a line-constraint with a fixed deformation value zero in the *x*-plane. The effect of this would cause a reduction in cross sectional area without compromising the unwanted kinematic behaviour of the specimen.

Next, the material specimen was analysed using the Neo-Hookean constitutive material law implemented in the SESKA framework was done. Figure 5-4 and table 5-2 exhibits an initial pseudo experimental material parameters, these pseudo experimental results will be compared to output parameters obtained from PODI analysis in section 5.2.3.

.

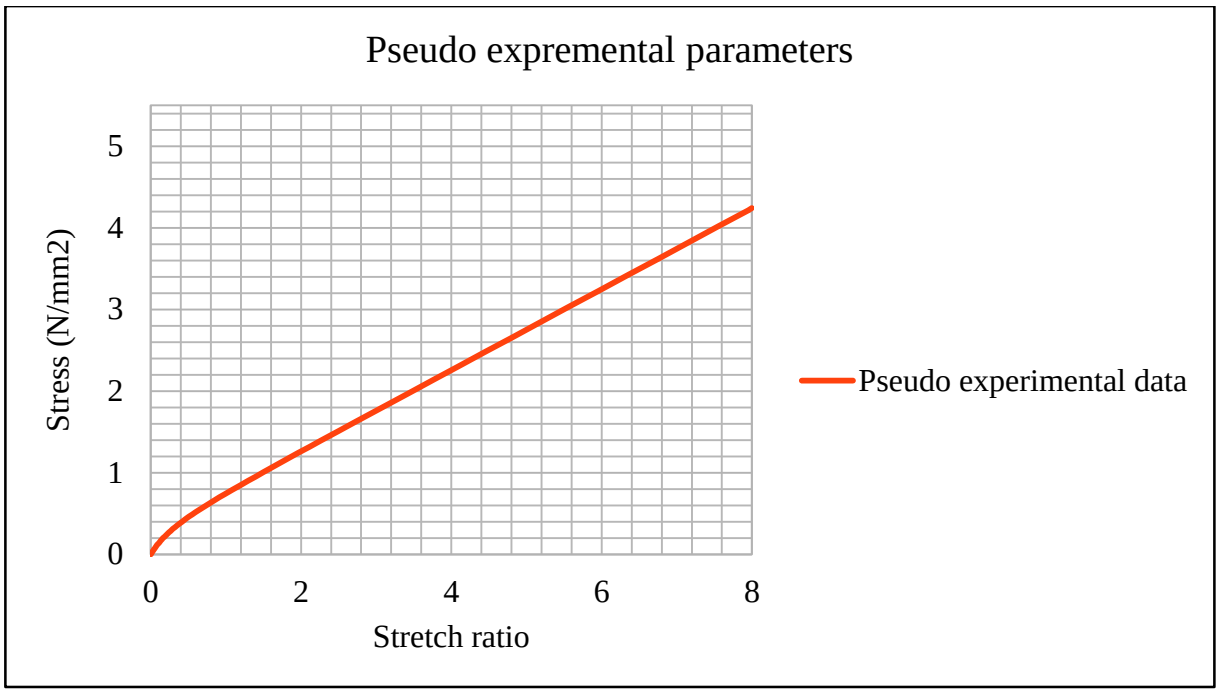

Figure 5-4: Initial material parameters

Table 5-2: Initial material parameters for a vulcanised rubber specimen

Parameter	Value (Dimensionless)
λ	125
μ	0.25

5.2.2 Database population

As mentioned in section 1.1.2, a requirement of the in-house POD-based software ORION is the need of a database of varying results corresponding to varying constitutive parameters. Table 5-3 illustrates the lower and upper limits of the aforementioned database. Moreover, to gain a better understanding of these limits, figure 5-5 graphically symbolises the upper and lower limits of the database proposed for a hyperelastic material.

Table 5-3: Range of database

	Limiting parameters in database	
	λ	μ
Upper limit	130	0.3
Lower limit	120	0.2

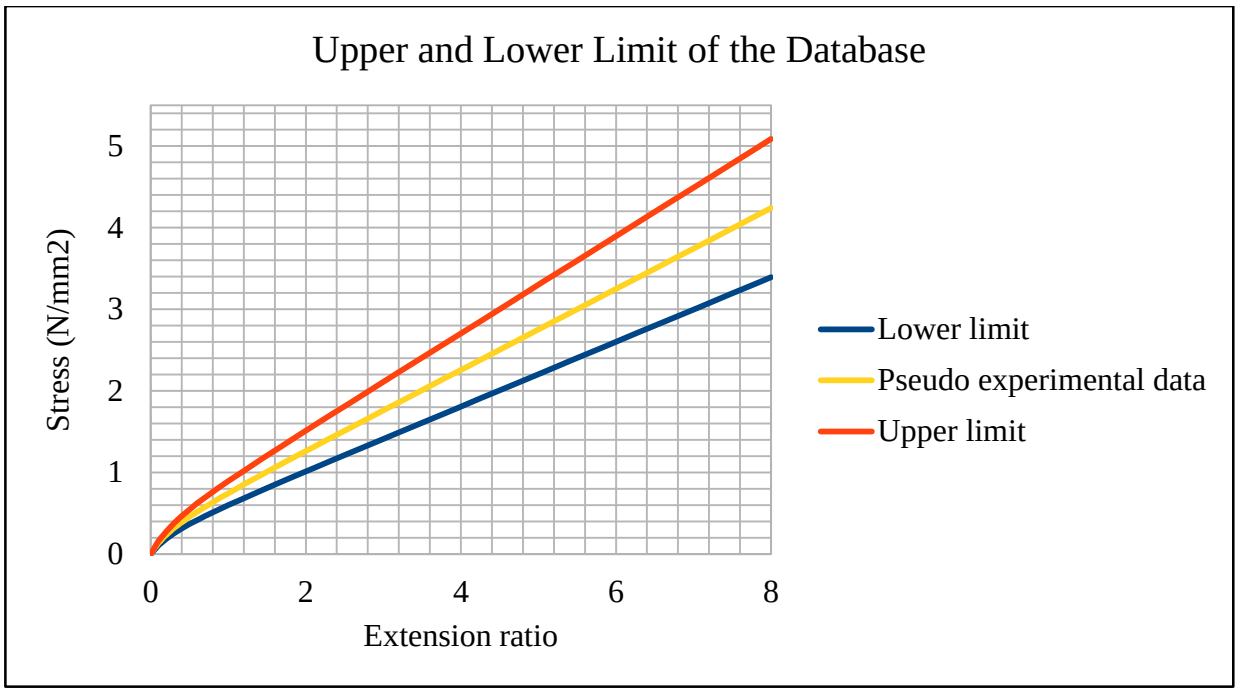

Figure 5-5: Graphical representation of limiting parameters

Table 5-4: Increments of parameters chosen to be calibrated

λ	μ
1.00	0.01

From tables 5-3 and 5-4, the author proposes that from a lower limit of 120, λ would increase in increments of 2.5 until it reaches the upper limit of 130. Additionally, μ would increase in increments of 0.01 from a lower limit of 0.2 up to value of 0.3. Consequently, populating a database comprised of 50 parameter combinations. Moreover, to gain a better understanding of the aforementioned database, figure 5-6 presents the reader with a graphical representation of the database

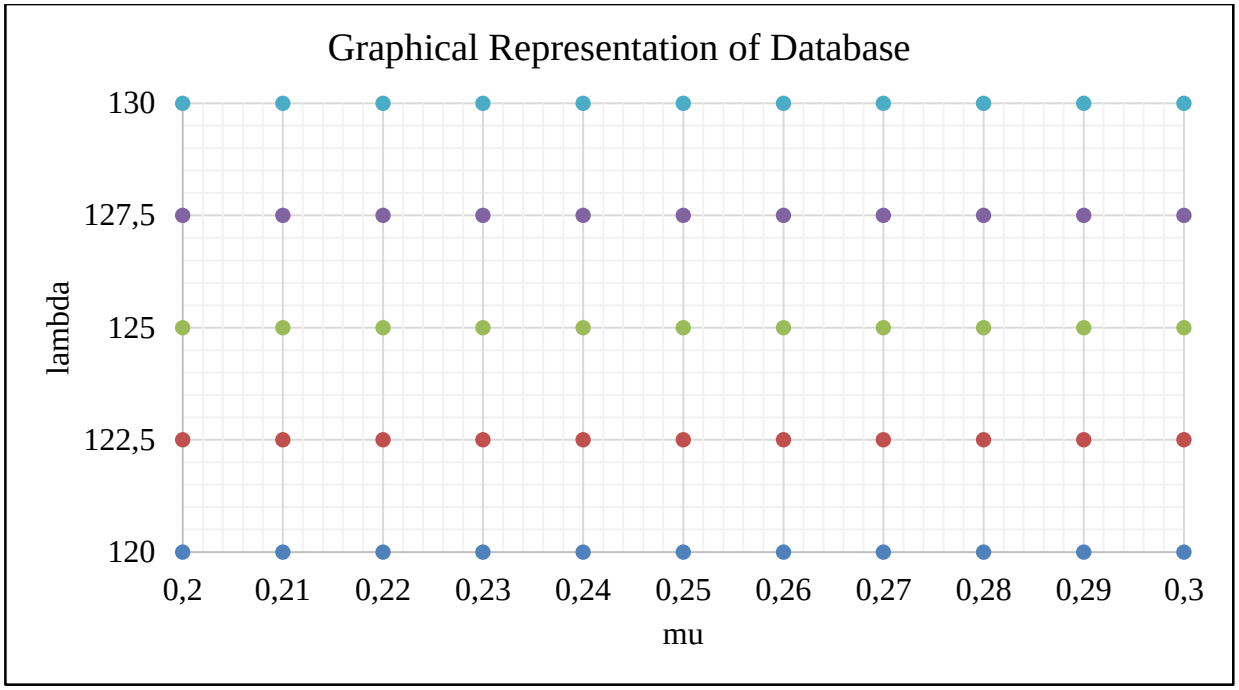

Figure 5-6: Graphical representation of database

5.2.3 Comparison between PODI and initial material constants

Once a database of varying constitutive parameters had been populated, it was analysed by coupling a MATLAB-based Levenberg Marquardt algorithm with the in-house POD-based software ORION. The results gathered from analysing the database was further examined using finite element software. In the following subsection, the author delineates the central theme of this research project, that being the time effectiveness of the PODI method. For this, the author will compare initial pseudo experimental results and output parameters obtained from PODI analysis. Furthermore, visual and numerical comparison between various constitutive relations would be presented in this section which would contribute to the fact that PODI could be used to obtain constitutive material parameters. Table 5-5 displays the evolution of the specimen's material parameters from initial input parameters until ORION and the Levenberg-Marquardt algorithm converges to final material parameters. In addition, Table 5-6 displays the error norm between initial pseudo experimental results and output parameters gathered form PODI analysis.

Table 5-5: Evolution of material parameters

Units N/mm^2	Evolution of material parameters	
	λ	μ
User defined initial parameters in ORION	122.5	0.21
Output parameters gathered from PODI analysis	125.235	0.25093

Table 5-6: Error norm of material parameters

Units N/mm^2	Error norm of material parameters	
	λ	μ
Pseudo experimental results	125	0.25
Output parameters gathered from PODI analysis	125.235	0.25093
Error	0.235	0.00093

Figures 5-7 and 5-8 provide a visual comparison between effective stress and strain between results gathered from the PODI results and the results gathered from using initial material constants. From these results, the author notes that the error in values presented in the aforementioned figures could be attributed to the interpolation method employed by ORION. Hence, the author notes that the size the database would affect the way ORION operates, if more data is available then the result would be more accurate.

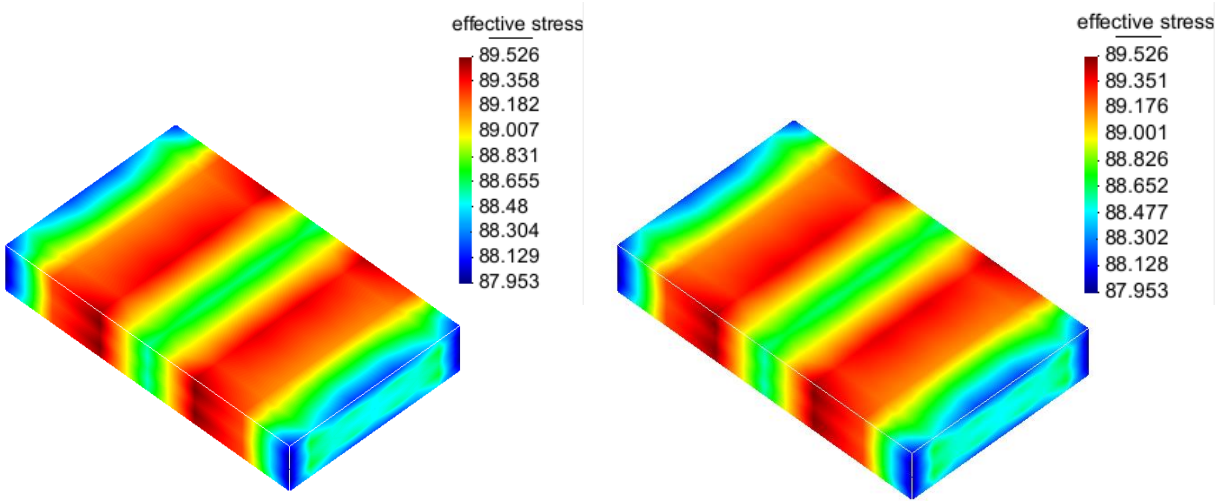

a) Pseudo experimental result b) PODI result

Figure 5-7: Comparison between effective stress measures in N/mm^2

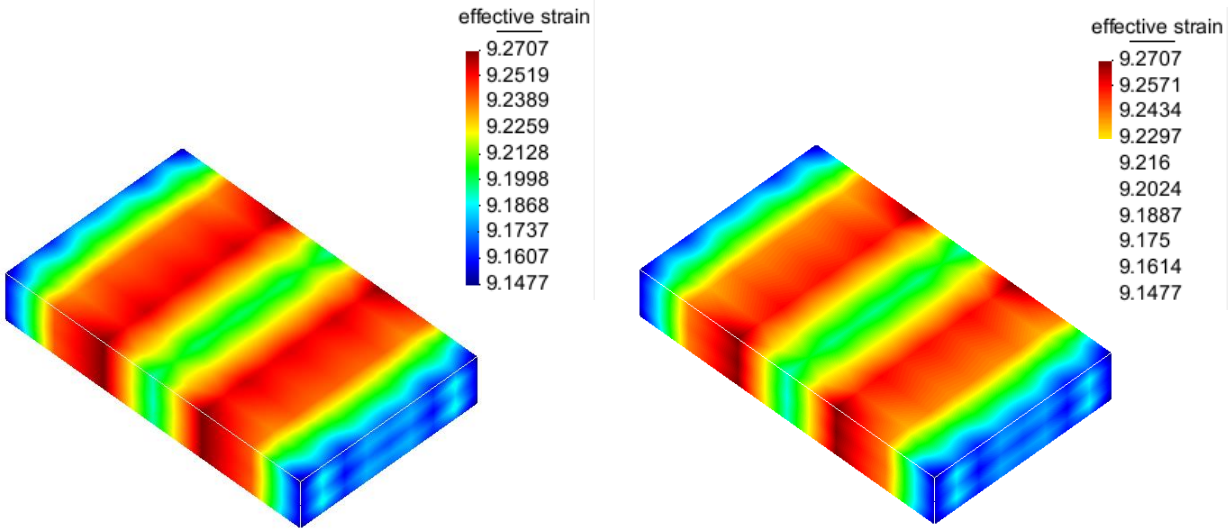

a) Pseudo experimental result b) PODI result

Figure 5-8: Comparison between effective strain measures

From visual and numerical comparison in figures 5-7 and 5-8, it could be seen that the error in values between PODI generated results and results obtained from initial material parameters appear to within an acceptable level. More importantly, it was noted that by coupling SESKA with the Levenberg-Marquardt algorithm took approximately 14 hours to produce a result. In contrast, coupling ORION with the Levenberg-Marquardt algorithm took approximately 30 minutes to produce results. Thus, it was noted that coupling ORION with the Levenberg-Marquardt algorithm would be an optimal method of computing constitutive material parameters.

5.3 Titanium specimen

5.3.1 Experimental setup

With regard to elastoplastic behaviour, the author analysed a cantilevered titanium specimen subject to a downward traction load at its free end. Figure 5-9 displays the geometry of the specimen analysed by the author, which was defined by a length of 10 000mm, a width of 1000mm, and a height of 1000mm. Figures 5-10 and 5-11 graphically depict how the author proposed to construct the cantilevered titanium specimen subject to a traction load at its free end. Additionally, the author notes that using particle displacement control constraint of 275 mm in the negative z-direction at the free end of the cantilevered specimen. This displacement constraint would provide the necessary control to prevent unwanted softening behaviour. The proposed specimen has been modelled using 283 mesh free, as shown in table 5-7.

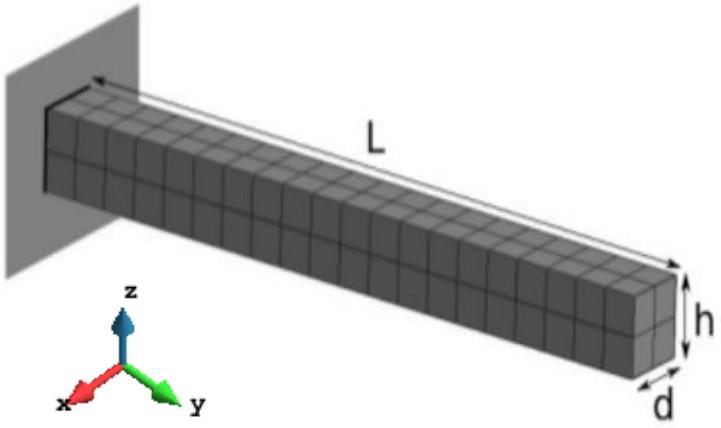

Figure 5-9: Geometry of material specimen (Essack, 2014)

Table 5-7: Discretized material meshed elements

Discretized materials meshed elements	
Element type	Number of elements
Linear elements	56
Quadrilateral elements	88
Hexahedra elements	40
Number of nodes	99
Total	283

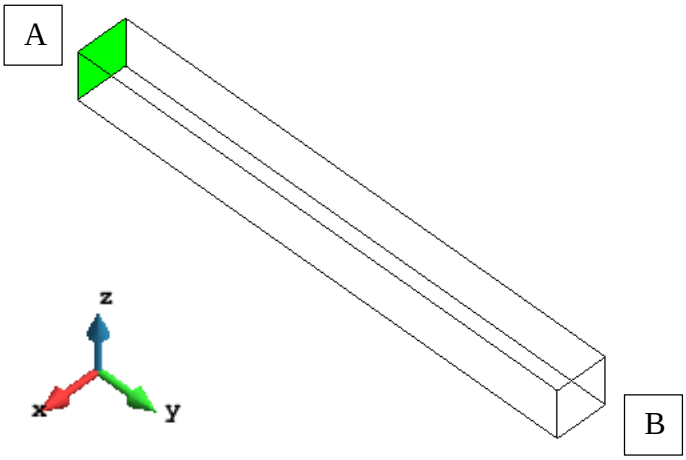

Figure 5-10: Dirichlet displacement surface-constraints

Considering Figure 5-10, the author applied a Dirichlet surface constraint at **A** with a value of zero in the *x*, *y*, and *z* direction respectively. This constraint would allow for no deformation of the surface to occur. Moreover, considering figure 5-11, the author applied a traction load in the negative z-direction as well as particle displacement control constraint at **B**, such that a deformation of 275 mm occurs at this end. The effect of coupling a traction load with a particle displacement control constraint would restrict excessive plastic behaviour.

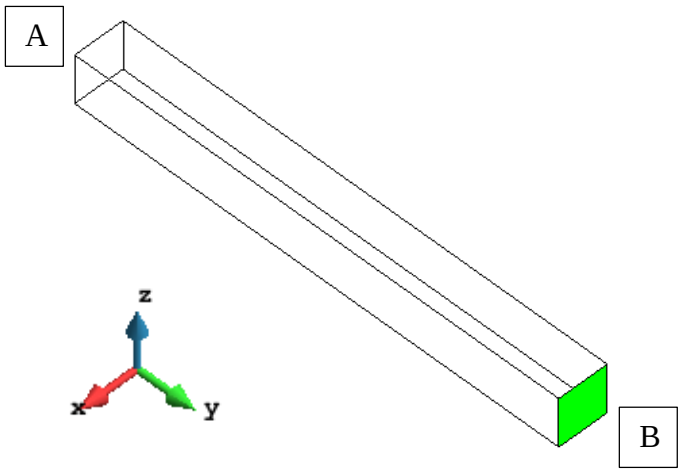

Figure 5-11: Traction load with a particle displacement control constraint

Next, pseudo experimental constitutive parameters had been analysed using the von Mises constitutive material law implemented in SESKA's framework. Figure 5-12 and table 5-8 display initial constitutive parameter constants, these pseudo experimental results will be compared to output parameters obtained from PODI analysis in section 5.3.3.

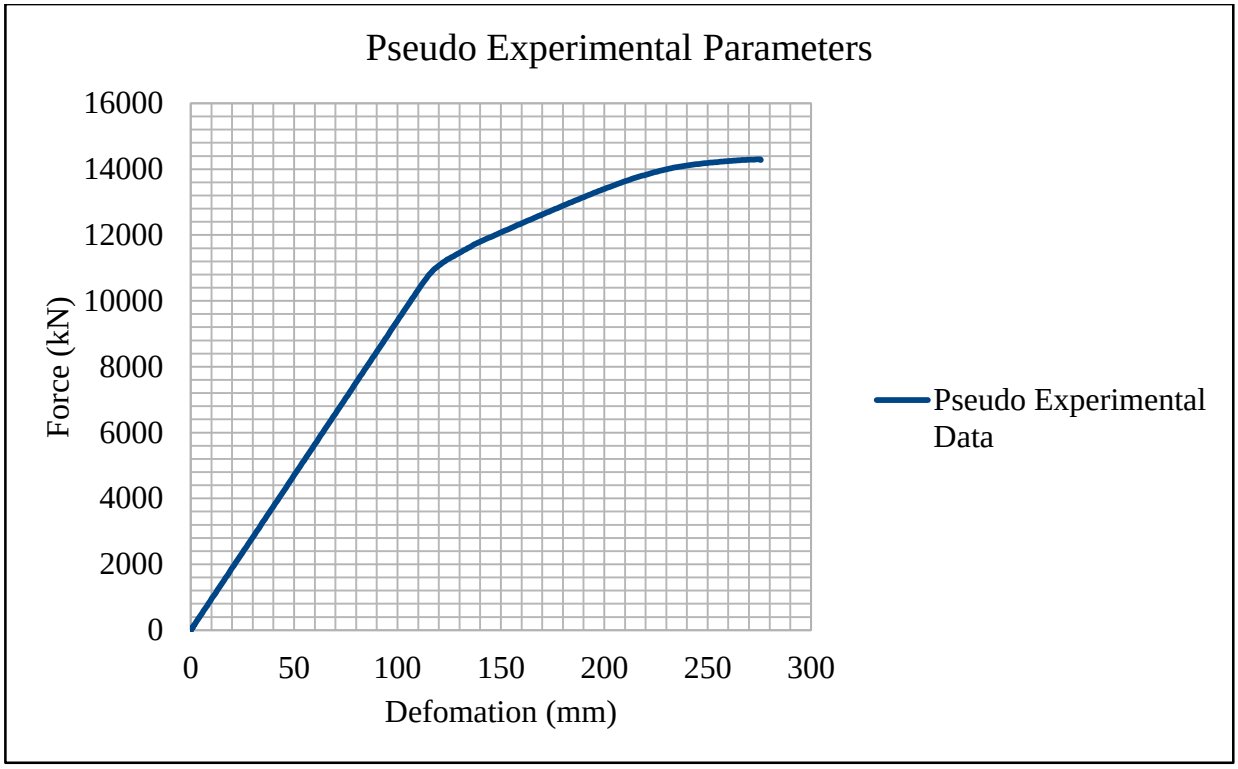

Figure 5-12: Initial material parameters

Table 5-8: Initial material parameters for a cantilevered titanium specimen

Parameter	Value (kN/mm^2)
μ	80.97
K	164.206
σ_y	0.450
σ_∞	0.715
H	0.129
η	16.92

In order to produce optimal FEM simulated constitutive results, the author used a step-wise approach. Firstly, the author utilized the von Mises constitutive material law to produce a desired elastic regime. Secondly, once the desired elastic regime could be achieved the author could then vary plastic parameters σ_∞ , H, and η in order to reproduce optimal pseudo experimental constitutive data.

5.3.2 Database population

Once again, a database of results corresponding to varying constitutive parameters needs to be populated in order to use the in-house POD-based software. In order to populate a database of results associated to varying constitutive parameters the author decided to vary plastic parameters rather than the elastic parameters. As a result, it could be said that the author varied non-linear parameters rather than linear parameters. Table 5-9 illustrates the upper and lower limit of the aforementioned database where σ_∞ , H, and η were the only parameters being varied. In contrast

to the database population of the vulcanized rubber specimen, the database of varying parameters of the titanium specimen would vary three parameters instead of two. In order to achieve this, each variation of σ_∞ would correspond to five variations of H, in addition to this each variation of H would correspond to three variations of η. Moreover, table 5-10 provides the reader with the numerical spacing constraints between the parameters being varied. Furthermore, figure 5-13 graphically displays the lower and upper limit of the aforementioned database.

Table 5-9: Range of database

Units kN/mm^2	Limiting parameters in database					
	μ	K	σ_y	σ_∞	H	η
Upper limit	80.97	164.206	0.450	0.615	0.06	8.46
Lower limit	80.97	164.206	0.450	0.815	0.175	25.38

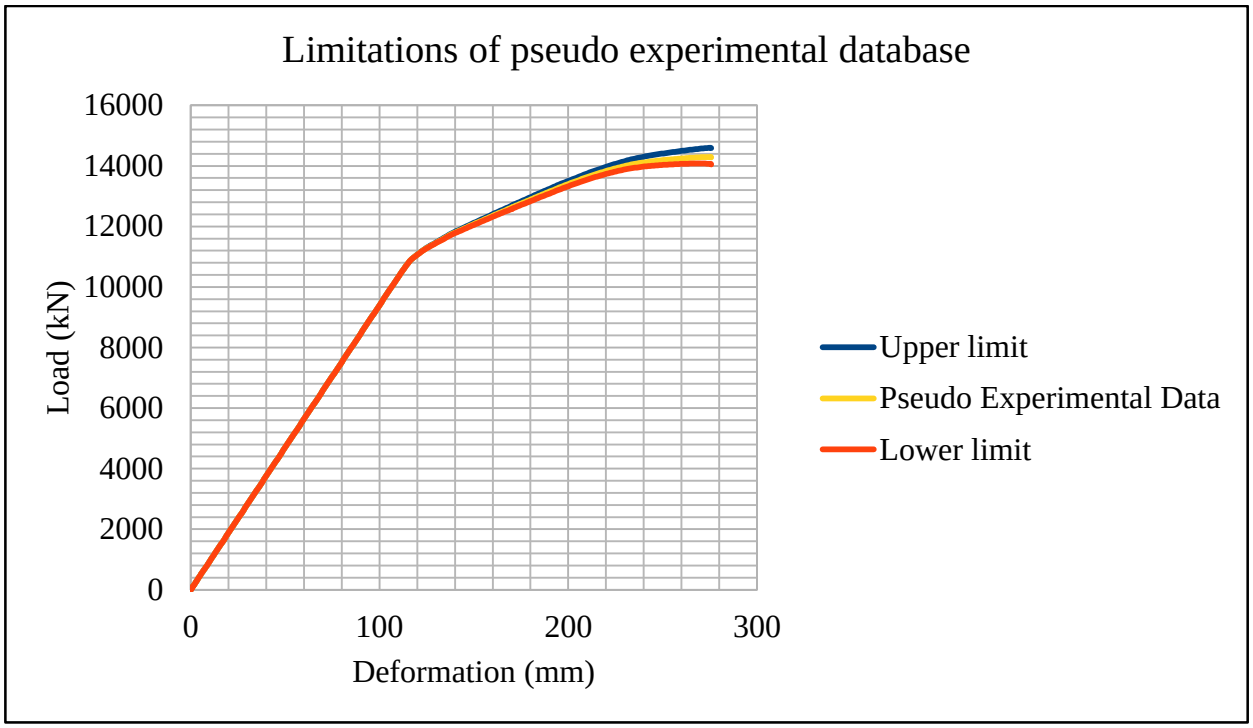

Figure 5-13: Graphical representation of limiting parameters

Table 5-10: Spacing of parameters chosen to be calibrated

σ_∞	H	η
0.05	0.05	8.46

Referring to tables 5-9 and 5-10, the author proposes that the σ_∞, H, and η would increase in increments of 0.05, 0.05, and 8.46 form their respective lower limits until they reach their respective upper limits. Consequently, populating a database comprised of 75 parameter

combinations. Moreover, to gain a better understanding of the aforementioned database, figure 5-14 presents the reader with a graphical representation of the database. Considering the same figure, the orange surface represents the initial material parameters for a cantilevered titanium specimen. Additionally, the red and dark purple surfaces represents the lower and upper limits of the database, respectively.

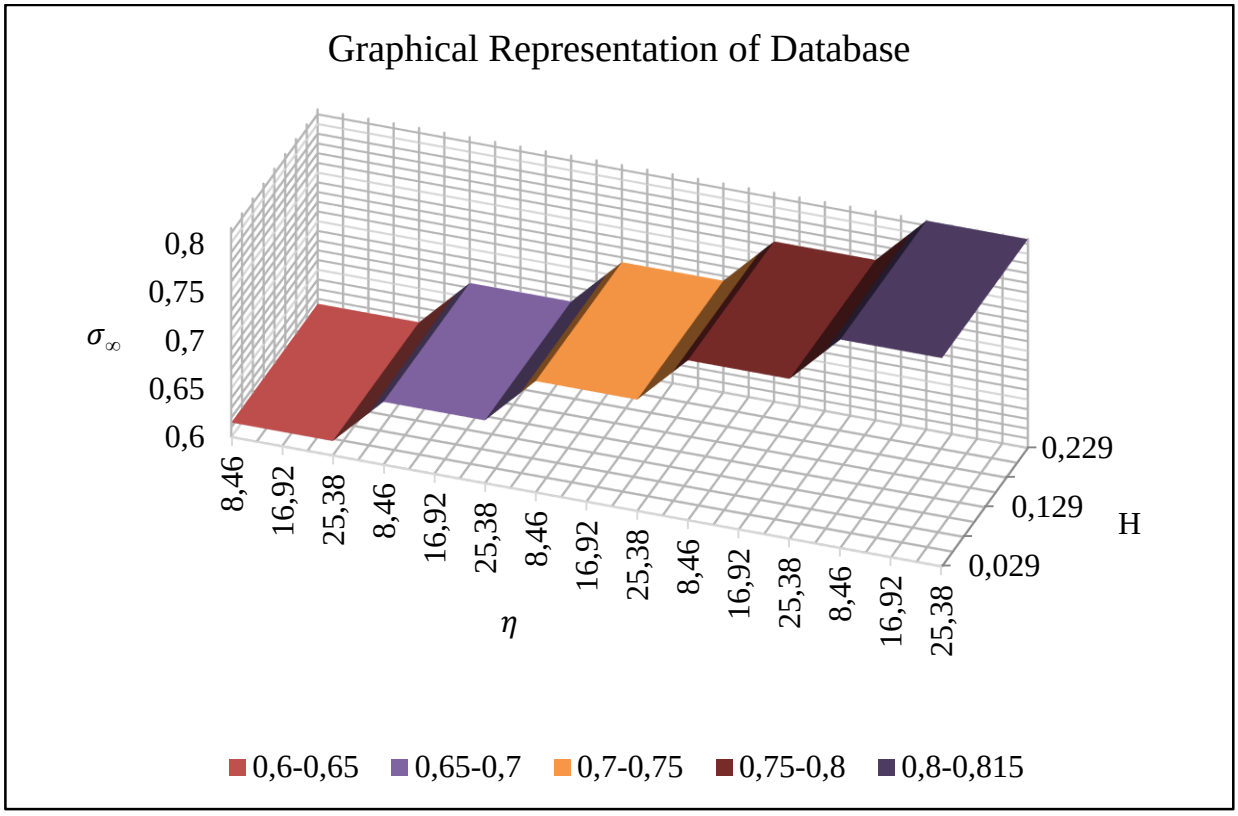

Figure 5-14: Graphical representation of Database

5.3.3 Comparison between PODI and initial material constants

Once the POD analysis was complete, the results gathered from ORION were analysed using finite element software. Similar to section 5.2.3, this section illustrates a visual and numerical comparison between effective stress and strain to contribute to the fact that PODI could be used to obtain constitutive material constants.

Since the database populated for the titanium specimen is larger than the database established for the natural rubber specimen, the author expected accurate results from the POD analysis. Table 5-11 displays the evolution of the specimen's material parameters from initial input parameters until ORION and the Levenberg-Marquardt algorithm converges to final material parameters.

Table 5-11: Evolution of material parameters

Units kN/mm^2	Evolution of material parameters					
	μ	K	σ_y	σ_∞	H	η
User defined initial parameters in ORION	80.97	164.206	0.450	0.665	0.079	8.46
Output parameters gathered from PODI analysis	80.97	164.206	0.450	0.724	0.138	16.922

Consequently, what was noted during analysis is that the evolution of the specimen's material parameters tend to oscillate around the final output parameters until the Levenberg-Marquardt algorithm reached a global minimum. This further cements the claim that the size of the database being populated not only has an effect on the accuracy of the PODI method but the evolution of material parameters as well. Table 5-12 illustrates the error between initial pseudo experimental results and Output parameters gathered from PODI analysis.

Table 5-12: Error norm of material parameters

Units kN/mm^2	Error norm of material parameters					
	μ	K	σ_y	σ_∞	H	η
Pseudo experimental results	80.97	164.206	0.450	0.715	0.129	16.92
Output parameters gathered from PODI analysis	80.97	164.206	0.450	0.724	0.138	16.922
Error	0	0	0	0.009	0.009	0.002

Additionally, Figures 5-15 and 5-16 illustrate a visual and numerical comparison between effective stress and effective plastic strain fields of PODI approximated results and results obtained from initial material constants.

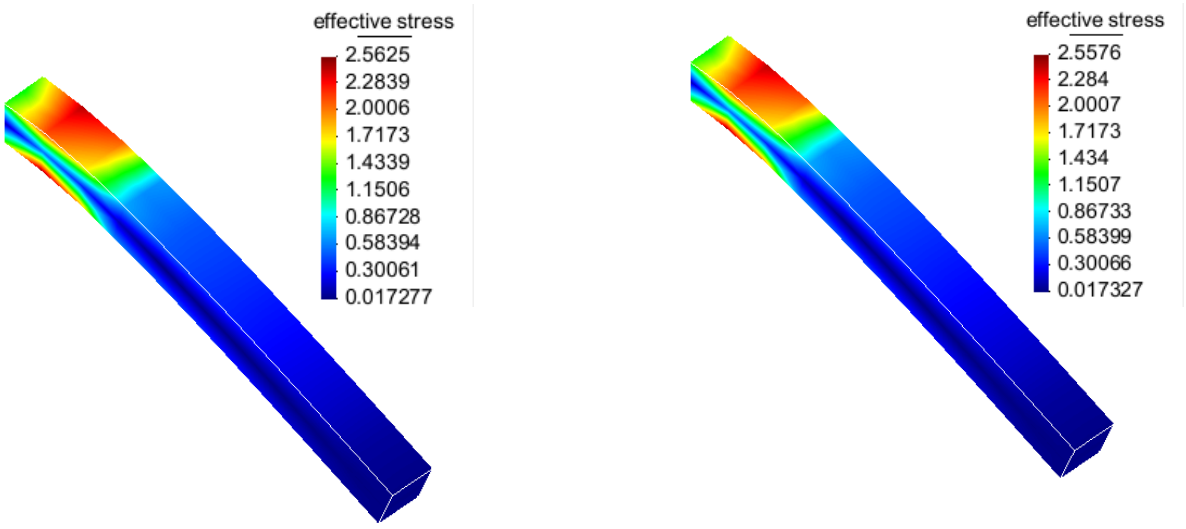

a) Pseudo experimental result b) PODI result

Figure 5-15: Comparison between effective stress fields in kN/mm2

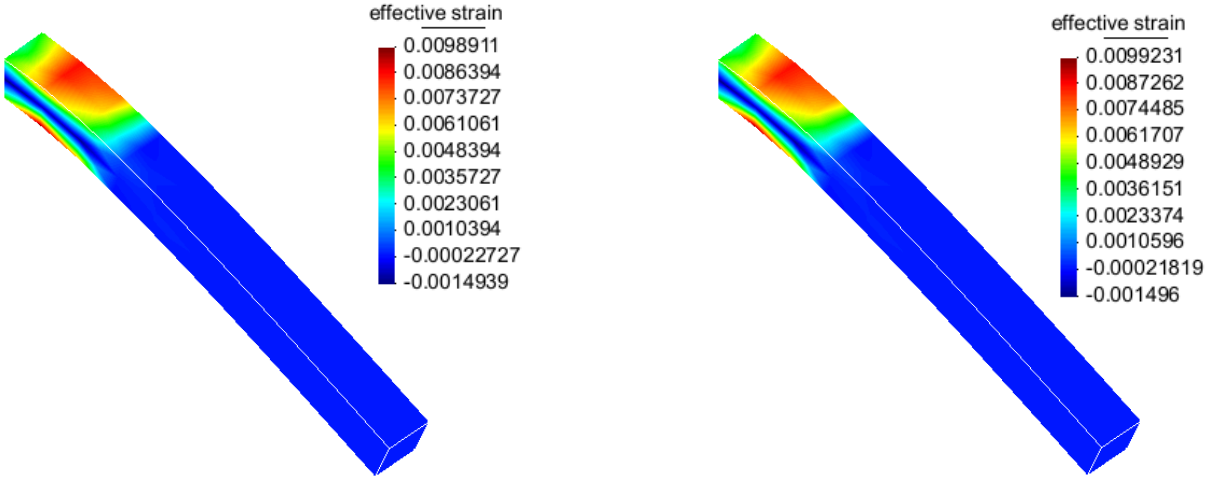

a) Pseudo experimental result b) PODI result

Figure 5-16: Comparison between effective plastic strain fields

Similar to the natural rubber specimen, the error in values presented in the aforementioned figures could be attributed to the interpolation method employed by ORION. However, from visual and numerical comparison in figures 5-15 and 5-16, it could be seen that the error in values between PODI generated results and results obtained from initial material parameters appear to within an acceptable level. More importantly, it was noted that by coupling SESKA with the Levenberg-Marquardt algorithm took approximately 2 hours to produce output results. In contrast, coupling ORION with the Levenberg-Marquardt algorithm took approximately 10 minutes to produce output results. Consequently, in contrast to the rubber specimen, the author notes that coupling ORION with the Levenberg-Marquardt algorithm could be used to analyse a more complicated material law in a time efficient manner.

6. Conclusions and recommendations

6.1 General remarks

Firstly, this document began by providing the reader with sufficient introduction into the work being investigated by the author. This introductory section provides the reader with a background, justification, and problem statement of the research project. Moreover, the aforementioned section provides a necessary outline of material parameter identification and a list of objectives that should be followed in order to complete this research project.

Secondly, this document provides the sufficient peer reviewed literature available regarding general material optimization techniques. Furthermore, it provides the reader with general descriptions and how non-linear constitutive material laws could be implemented to achieve the ultimate objective of Proper Orthogonal Decomposition-based Material Parameter Optimization.

Finally, this document outlines computational mechanics theory relevant to this work. This includes the provision of kinematic balance laws important to this work. Furthermore, this section provides appropriate equations that could be used to construct general constitutive material laws. Moreover, the provision of hyperelastic and elastoplastic constitutive material equations further cements the fact that a computational approach rather than an analytical approach should be used to investigate the constitutive behaviour of non-linear constitutive behaviour.

6.2 Identification of material parameters

With regard to calibrating a hyperelastic material, with reference to section 5.2, the following conclusions could be made. Firstly, in order to calibrate accurate constitutive material constants, the need for a well-defined experimental set up was found to be at the crux of the accuracy of the PODI method. The minor errors in accuracy of constitutive values presented in section 5.2 further cements that PODI could be used to effectively model the mechanical behaviour of rubber specimens.

With regard to calibrating the elastoplastic material, with reference to section 5.3, the following conclusions could be made. Once a hyperelastic material was successfully analysed, the author noted that the size of the database of results corresponding to various material parameters had an effect on the accuracy of the PODI method. Moreover, it was noted that the increments at which parameters are varied would also have an effect on the sensitivity of the PODI method. Consequently, the size of the database populated for the elastoplastic material was larger than that of the rubber specimen analysed in section 5.2, which resulted in improved accuracy of the PODI method. Equally important, the author notes that the use of the PODI method employed by ORION significantly reduced the time it takes to produce results, whether these results are positive or negative. Coupling the Levenberg-Marquardt algorithm with the PODI method, results gathered from the hyperelastic material were produced 96.43% faster than coupling the same algorithm with SESKA. Additionally, results gathered from the elastoplastic material were produced 91.67% faster when coupling the Levenberg-Marquardt algorithm with

the PODI method than coupling the same algorithm with SESKA.

6.3 Further use

Positive results were gathered form the analyses of hyperelastic and elastoplastic constitutive material laws. The premise that simulation time would increase as the complexity of the constitutive law being investigated increases brought forward the use of POD-based software could be used to decrease simulation. However, it should be noted that user specific alterations need to be made to the Levenberg-Marquardt algorithm before successful commercial use could be implemented in the future.

7. References

Andriyana, A., 2008. Failure Criteria for Yielding. Sophia Antipolis: Centre de Mise en Forme des Mat´eriaux.

Batra, R. C., 1998. Linear Constitutive Relations in Isotropic Finite Elasticity. Journal of elasticity, 51(3), pp. 243-245. DOI: 10.1023/a:1007503716826

Bigoni, D., 2012. Nonlinear Solid Mechanics. 1st ed. New York: Cambridge University Press. ISBN: 9781107025417

Bower, A., 2009. Applied mechanics of solids. 1st ed. United States of America: CRC Press. ISBN: 9781439802472

Coleman, T., Branch, M. A. & Grace, A., 1999. Optimization Toolbox for use with MATLAB, Natick: The MathWorks, Inc.

Dasgupta, K., 2014-2015. Virtual work lecture notes. Guwahati: Indian Institute of Technology Guwahati.

Department of Chemistry and Biochemistry, University of Colorado Boulder, 2015. Colorado Chemistry Lecture Demonstration Manual. [Online]
Available at: https://chem.colorado.edu/genchemdemo/index.php/thermochemistry/t590-enthropy-stretching-rubber-bands
[Accessed 17 July 2015].

Eberhart, R. & Kennedy, J., 1995. A New Optimizer Using Particle Swarm Theory, Purdue: Purdue School of Engineering and Technology. DOI: 10.1109/MHS.1995.494215

Essack, M. A., 2014. Material Parameter Identification for Modelling the Left Ventricle in the Healthy State, Cape Town: University of Cape Town.

Falkiewicz, N. J. & Cesnik, C. E., 2011. Proper orthogonal decomposition for reduced-order thermal solution in hypersonic aerothermoelastic simulation. AIAA Journal, 49(5), pp. 994-1009. DOI: AIAA-2010-2798

Gavin, H. P., 2011. The Levenberg-Marquardt method for nonlinear least squares curve fitting problems, Duke: Duke University.

Gennert, M. A. & Yuille, A. L., 1998. Determining the Optimal Weights in Multiple Objective Function Optimization, Worcester: Worcester Polytechnic Institute Research Development Council. DOI: 10.1109/ccv.1988.589974

Guo, Z. & Sluys, L. J., 2008. Constitutive modelling of hyperelastic rubber-like materials, Delft: Heron. ISSN: 0046-7316

Hashiguchi, K., 2009. Elastoplasticity theory. Heidelberg: Springer. DOI: 10.1007/978-3-642-00273-1_11

Haupt, P., 2000. Continuum mechanics and theory of materials. 1st ed. New York: Springer. ISBN: 978-3-662-04111-6, 978-3-662-04109-3

Hibbeler, R. C., 2008. Mechanics of Materials. 7th ed. Singapore: Pearson Education South Asia Pte Ltd.

Hopkins, G., 2014. Highly non-linear post-buckling analysis of shell structures, Cape Town: University of Cape Town.

Hui, Y., Liang, W., Hong-yuan, J. & Ulannov, A., 2010. Research on the mechanical performance parameter of Metal Rubber, Harbin: WASE International Conference on Information Engineering. DOI: 10.1109/ICIE.2010.207

Ishibuchi, H. & Murata, T., 1999. Local Search Procedures in a Multi-objective Genetic Local Search Algorithm for Scheduling Problems, Osaka: Osaka Prefecture University. DOI: 10.1109/ICSMC.1999.814171

Jin, X., Fourcaud, T., Li, B. & Guo, Y., 2010 IEEE. Plant Growth Modelling and Applications. Towards Modelling and Analysing Stem Lodging for Two Contrasting Rice Cultivars, pp. 253-260. DOI: 10.1109/PMA.2009.16

Kanzow, C. & Petra, S., 2005. LMMCP - A Levenberg-Marquardt-type MATLAB Solver for Mixed Complementarity Problems, Wurzberg: University of Wurzberg.

Kerschen, G., Golinval, J-C., Vakakis, A.F. and Bergman, L.A. The method of proper orthogonal decomposition for dynamical characterisation and order reduction of mechanical systems: An overview. Nonlinear Dynamics, 41:147(169, 2005). ISSN: 0924-090X

Kim, J. H. et al., 2007. Development of Nonlinear Constitutive Laws for Anisotropic and Asymmetric Fibre Reinforced Composites. Polymer Composites, pp. 216-228. ISSN: 0272-8397

Kim, N.-h., 2015. Introduction to non-linear finite element analysis. 1st ed. London: Springer. DOI: 10.1007/978-1-4419-1746-1

Li, H., Luo, Z. & Chen, J., 2011. Numerical simulation based on POD for two dimensional solute transport problems. Applied Mathematical Modelling, 35 (5), pp. 2489-2498. DOI: 10.1016/j.apm.2010.11.064

Lin, W. Z. & Zhang, Y. J., 2008. IEEE Transactions on Advanced Packaging. Proper Orthogonal Decomposition in the Generation of Reduced Order Models for Interconnects, 31(3), pp. 627-636. DOI: 10.1109/tadvp.2008.927820

Lourakis, M. I., 2005. A Brief Description of the Levenberg-Marquardt Algorithm Implemented, Heraklion, Crete, Greece: Levmar.

Mase, G. T. & Mase, G. E., 1999. Continuum mechanics for engineers. 2nd ed. Boca Raton: CRC press. ISBN: 9780849318559

Moosebrugger, C., 2002. Atlas of stress-strain curves. 2nd ed. United States of America: ASM International. ISBN: 0-87170-739-X

Nath, M. M., 2015. Quora. [Online]
Available at: https://www.quora.com/I-am-using-Hypermesh-as-a-preprocessor-for-finite-element-analysis-How-do-I-decide-which-element-to-use-and-on-what-basis-is-this-decided
[Accessed 15 September 2015].

Neaken, A., 2004. An as-short as possible introduction to the least squares, weighted least squares and moving least squares methods for scattered data approximation and interpolation, Darmstadt: Discrete modelling group.

Neto, E. D. S., Peric, D. & Owen, D., 2008. Computational analysis for plasticity - theory and applications. 1st ed. Swansea: Wiley & sons. ISBN: 9780470694633

Nexans, 2009. Nexans. [Online]
Available at: http://www.nexans.ru/Korea/2009/graph_cold_cable_500.jpg
[Accessed 20 September 2015].

Oden, J. T., 2008. Non-linear continuum mechanics. Introduction to mathematical modelling, September, p. 69. ISBN: 0-9614088-0-4

Oden, J. T. & Ripperger, E. A., 1981. The energy principles. 2nd ed. Washington: Hemisphere Publications; McGraw-Hill. ISBN: 0-07-047507-5

Otieno, M., 2012. Introduction to virtual work lecture notes. Cape Town: University of Cape Town.

Rama, R. R. & Skatulla, S., (Not Published). Real-time modelling of the heart using proper orthogonal decomposition with interpolation, Cape Town: University of Cape Town.

Reddy, J. N., 2015. An introduction to nonlinear finite element analysis. 2nd ed. New York: Oxford University Press. ISBN: 9780198525295

Rice, J. R., 2010. SOLID MECHANICS, Cambridge: Harvard University.

Runesson, K., 2006. The Primer. Constitutive Modelling of Engineering Materials - Theory and Computation, (Seventh Revised Edition), p. 2013. ISSN: 0020-7683

Sanchez, L. G. M., 2003. Use of Non-linear Constitutive Models in the Absolute Nodal Coordinate Formulation, Seville: University of Seville. UMI Number: 3316752

Sansour, C. & Kollman, F. G., 1997. On theory and numerics of large viscoplastic deformation. Computational methods in applied mechanics and engineering, 140(4), pp. 351-369. DOI: 10.1016/s0045-7825(96)01235-2

Savic, D., 2002. Single-Objective vs. Multiobjective Optimisation for Integrated Decision Support, Exeter: University of Exeter.

Sirovich, L., 1987. Turbulence and the dynamics of coherent structures. Quarterly of applied mathematics, XLV(3), pp. 561-571. ISSN: 0033-569X

Stolfi, J., 2013. Wikimedia Commons. [Online]
Available at: https://commons.wikimedia.org/wiki/File:Isotropic_stress_noavg.svg
[Accessed 27 September 2015].

Taber, L. A., 2004. Constitutive Relations. In: L. A. Taber, ed. Nonlinear theory of Elasticity - Applications in Biomechanics. Singapore: World Scientific Publishing, pp. 145-243. DOI: 10.1142/9789812794222_0006

The Mathworks, I., 2015. MathWorks. [Online]
Available at: http://www.mathworks.com/help/matlab/index.html
[Accessed 22 June 2015].

Treloar, L. R., 1943. Stress-strain data for vulcanised rubber under various types of deformation. London, Gurney and Jackson, pp. 59-70. DOI: 10.1039/tf9444000059

Treloar, L. R., 2005. The Physics of Rubber Elasticity. 3rd ed. Oxford: Clarendon Press. ISBN: 9781435609747

University of Cambridge, 2015. DoITPoMS. [Online]
Available at: http://www.doitpoms.ac.uk/tlplib/metal-forming-1/yield_criteria.php
[Accessed 10 September 2015].

University, B., 2015. Continuum Mechanics. [Online]
Available at:
http://www.brown.edu/Departments/Engineering/Courses/En221/Notes/Elasticity/Elasticity.htm
[Accessed 25 September 2015].

William, K. J., 2002. Encyclopedia of Physical Science & Technology. Constitutive Models for Engineering Materials, 3(Third Edition), pp. 603-633.

World, R., 2015. Revision World. [Online]
Available at: http://revisionworld.com/a2-level-level-revision/physics/force-motion/solid-materials/rubber
[Accessed 17 July 2015].

Zang, A. & Stephansson, O., 2010. Stress fields of the earths crust, s.l.: Springer Science+Business Media. ISBN: 9781402084430